Homogenates were frozen (-80°C) and thawed twice and then centrifuged for 10 min at 13,000 × *g* at 4°C. The total protein content of the supernatants was determined by the Bradford method with protein assay dye reagent (Bio-Rad, Hercules, CA, USA) with calibration using bovine serum albumin (Sigma-Aldrich). For the luciferase assay, 10 μL of supernatant homogenate was mixed with 50 μL of luciferase assay reagent II (Promega), and luciferase activity was measured by a luminometer (Lumat LB9507; Berthold Technologies, Bad Wildbad, Germany). The data were presented as the relative light units per total protein content.

Detection of Lac Z protein

For visual confirmation of the gene expression in each organ, 20 μg of pCAGGS-Lac Z and the same dose of pCAGGS, as a control, were introduced. 48 h after the hydrodynamic injection, mice were sacrificed and each organ (liver and lung) was excised and fixed with a mixture of 0.2% (v/v) glutaraldehyde and 1% (v/v) formaldehyde for 1 h at 4°C, and the samples were then stained with 1 $mg \cdot mL^{-1}$ of 5-bromo-4-chloro-3-indolyl-β-D-galactopyranoside (X-gal; Sigma-Aldrich).

ST2-overexpressing mice

In order to prepare ST2-overexpressing mice, pCAGGS-mST2 was introduced by hydrodynamic injection, and pCAGGS was used as a control. Starting 12 h after the gene transfer, blood was collected from the tail vein and the concentration of plasma ST2 protein was confirmed. Concurrently, bronchoalveolar lavage fluid (BALF) and lung homogenate were prepared for examining the ST2 protein in the lung. Lavage was performed under deep anaesthesia with a lethal dose of pentobarbital, and the trachea was cannulated with an 18-gauge catheter. The lungs were inflated with 1 mL of cold sterile saline, the solution was slowly recovered and centrifuged at 400 × *g* for 10 min at 4°C, and the resultant supernatant was collected and analysed. ~0.8 mL of BALF was consistently recovered, and therefore this amount was used to determine the content of ST2 protein in BALF. To obtain the lung homogenate, the remaining mice were anaesthetised, as described previously, and perfusion of pulmonary vessels with 5 mL saline was carried out *via* the right ventricle. The lungs were then excised and homogenised in 2 mL cold saline using a Polytron homogenizer (Kinematica) on ice. The resultant solution was centrifuged at 9,000 × *g* for 15 min at 4°C, and the supernatant was subjected to analysis. The concentrations of ST2 protein in plasma, BALF and lung homogenate were measured by ELISA.

mST2 ELISA

The mST2 ELISA system was originally constructed in our laboratory, as previously described [7]. Briefly, the bottom of a 96-well ELISA plate (Sumitomo Bakelite Co., Tokyo, Japan) was coated with rat monoclonal antibody against mouse T1/ST2 protein (MD Biosciences, Zurich, Switzerland) and samples were added and incubated for 1 h at room temperature. Next, rabbit anti-mST2 polyclonal antibody [12] and HRP against rabbit IgG (GE healthcare UK Ltd, Chalfont St Giles, UK) were added consecutively. Finally, O-phenylenediamine solution was used as substrate and optical density was measured at 450 nm with a microplate reader (Inter Medical, Tokyo, Japan).

Induction of bleomycin-induced lung injury

Mice were anaesthetised by intraperitoneal injection of pentobarbital (50 $mg \cdot kg^{-1}$), then 50 μL of bleomycin (Nippon Kayaku Co., Tokyo, Japan) dissolved in sterile saline was administered intratracheally, as previously reported [15]. To determine the appropriate dosage of bleomycin, bleomycin was administered preliminarily at different doses, 2.5 and 1 $mg \cdot kg^{-1}$ to mice. In the 2.5 $mg \cdot kg^{-1}$-injected group, body weight decreased rapidly, and almost all animals died between days 7–10. Conversely, in the 1 $mg \cdot kg^{-1}$-injected group, about half of the mice remained alive. Therefore, it was established that the optimal bleomycin dose for our purpose was 1 $mg \cdot kg^{-1}$.

In plasmid-introduced mice, at 24 h after gene transfer (pCAGGS and pCAGGS-mST2) to mice, blood was sampled from the tail vein and the level of ST2 protein was determined. After an additional 24 h, as controls, the same volume of saline or the same dose of bleomycin was administered to mice after hydrodynamic injection with the same volume of saline (6.3% of the total body weight) without plasmid vectors.

Reverse transcriptase-PCR analysis

Bleomycin-induced mRNA expression of several cytokines and mST2 was examined by reverse transcriptase (RT)-PCR analysis. Mice that had not undergone gene transfer were administered bleomycin intratracheally, and after 1, 3 or 7 days, the whole lungs were removed and immediately immersed in 1 mL of TRI reagent (Sigma-Aldrich). After homogenisation with a Polytron homogeniser (Kinematica), total RNA was extracted and purified according to the manufacturer's protocol. Contaminated genomic DNA was destroyed by DNase I (Takara, Shiga, Japan), and cDNAs were synthesised using moloney murine leukaemia virus RT (Invitrogen, Carlsbad, CA, USA). The nucleotide sequence of the primers used were as follows. mST2: (forward) 5′- GCGG-AGAATGGAACCAACTA-3′, (reverse) 5′-CAATGTGTGAGG-GACACTCC-3′; β-actin: (forward) 5′- TGTCCCTGTATGCC-TCTGGTA-3′, (reverse) 5′-ACTGTGTTGGCATAGAGGTC-3′; tumour necrosis factor (TNF)-α: (forward) 5′- CTGGGCAGG-GGCCACCACGCTC-3′, (reverse) 5′-CTCAGCGCTGAGTTG-GTCCCCCTTCTC-3′; IL-1β: (forward) 5′- GCTGCTTCCAAA-CCTTTGAC-3′, (reverse) 5′-AGGCCACAGGTATTTTGTCG-3′; and IL-33: (forward) 5′-ATGAGACCTAGAATGAAGTATT-CCA-3′, (reverse) 5′-TTAGATTTTCGAGAGCTTAAACATA-3′. 10 μL of PCR products were developed by electrophoresis on 1% agarose gels, and the gels were stained with ethidium bromide.

Measurement of cytokines and albumin in BALF

After the treatment with bleomycin, the lungs were lavaged four times with 0.7 mL of cold PBS. After lavage, the total number of cells was immediately counted and the cell type was identified. For the determination of cell types, cells obtained through centrifugation in a cytospin at 120 × *g* for 10 min were stained with Diff-Quick (Sysmax, Kobe, Japan). The remaining BALF was centrifuged at 400 × *g* for 10 min at 4°C, and the supernatant was analysed. The concentrations of cytokines (TNF-α, IL-1β and IL-6) in BALF were measured using ELISA kits (Biosource, Camarillo, CA, USA), and albumin concentration was measured by a turbidimetric

immunoassay using R-ALB-UR (Kyokuto Pharmaceutical Industrial Co., Tokyo, Japan). Bronchoalveolar lavage (BAL) was performed four times with 0.7 mL PBS, and ~2.5 mL was continually recovered in each case.

Histology

Mice were sacrificed and pulmonary vessels were perfused with 5 mL of saline *via* the right ventricle. Then, after intratracheal injection of 1 mL of 10% (v/v) neutral formalin buffered with 0.2 M cacodylate solution (pH 7.4), the lungs were excised and post-fixed with the same fixative for 10 h and were embedded in paraffin. Sections were cut into 6-μm thick slices, which were stained by haematoxylin and eosin (H&E) solution and Mallory–Azan.

To quantify the histological findings, the tissue volume density (TVD) was calculated using Scion Image software (Scion Corporation, Frederick, MD, USA), and the proportion of airspace consolidation and atelectasis to the total areas was obtained.

Analysis of body weight loss and survival after bleomycin treatment

24 h after hydrodynamic gene transfer (pCAGGS and pCAGGS-mST2), bleomycin was administered intratracheally (1 $mg \cdot kg^{-1}$). Over 14 days following gene transfer, the mortalities and body weights in each group of mice were monitored.

Statistical analysis

The data are presented as mean±SD. Statistical analyses were performed by an unpaired t-test (comparing two groups) or by ANOVA followed by the Tukey's test (comparing multiple groups), and survival analysis was performed using the Kaplan–Meier method. SPSS 11.0J (SPSS Inc., Chicago, IL, USA) was used for each statistical analysis. p-values <0.05 were considered statistically significant.

RESULTS

Hydrodynamic gene transfer

Hydrodynamic injection, a strategy used to transfer naked plasmid DNA into animals, was applied to obtain ST2-overexpressing mice. First, in order to confirm the overexpression of the transgene by hydrodynamic injection, we injected the pGL3 control vector into the mice, and observed the luciferase expression *in vivo* (fig. 1a). Luciferase expression was most prominent around the upper abdomen, and was significantly elevated at day 1. No specific signals were detected in the saline-injected mice.

Next, to confirm the transgene expression in each organ, several organs (the liver, lung, heart, kidney and spleen) were excised and the luminescence activity was measured after hydrodynamic gene transfer of the pGL3 control vector. Figure 1b and c demonstrate that the liver showed outstanding luminescence activity, and thus, the liver is the only target organ of this gene transfer method. The other organs from the pGL3-injected mice showed lower luminescence activity than the liver, but higher activity than that of control mice. Furthermore, to detect transgene expression visually, pCAGGS-LacZ was administered in the same manner, and the liver and lung were excised and stained with X-gal solution. As shown in figure 1d, the liver was clearly stained blue; however, there was almost no detectable β-galactosidase expression in the lung (fig. 1e). This outcome corresponded to the results of the bioluminescent assay.

Transient overexpression of mST2 protein

Before *in vivo* application, to confirm the production of mature mST2 protein from the constructed plasmid, pCAGGS and pCAGGS-mST2 were transferred into HEK 293T cells. The culture supernatant was collected for Western blotting. As shown in figure 2a, both the glycosylated mature form of ST2 (60–70 kDa) and the core peptide (37 kDa) obtained by digestion with *N*-glycosidase F were clearly detected. The results indicated that the mature ST2 protein was appropriately expressed and secreted from the cultured cells using our constructed plasmid.

We then carried out *in vivo* gene transfer into mice using hydrodynamic injection. First, we determined the appropriate amount of plasmid for obtaining the maximum plasma concentration of the ST2 protein. As shown in figure 2b, various amounts of plasmid vectors (10–100 μg) were introduced, and the concentration of plasma ST2 protein increased significantly in accordance with the amount of plasmid administered. It reached a maximum level when 50 μg of the plasmid was injected, but no significant increase was observed when the amount of plasmid was increased from 50 to 100 μg. Therefore, the amount of the plasmid was fixed at 50 μg for the subsequent *in vivo* experiments.

The time-kinetics of the introduced ST2 protein were examined next. As shown in figure 2c, the ST2 protein level in plasma attained a peak at ~12–24 h (18.1–27.6 $\mu g \cdot mL^{-1}$) and gradually decreased until 21 days (4.07 $\mu g \cdot mL^{-1}$). Empty vector-injected mice showed no increase in ST2 level from the beginning to the end of the trial, indicating that the injection of plasmids itself did not exert any influence on the endogenous ST2 level. For examination of the level of local ST2 protein in the lung, 1 mL of saline was injected intratracheally to obtain BALF, and almost constant recovery of 0.8 mL was obtained. The level of BALF ST2 protein was 10.81 ± 3.31 $ng \cdot mL^{-1}$, as measured by ELISA, and therefore the BALF ST2 protein content was estimated at 8.65 ± 2.65 $ng \cdot BALF^{-1}$. To collect lung homogenate, the lungs were excised and homogenised in 2 mL of saline. Since the concentration of ST2 protein was 23.57 ± 12.72 $ng \cdot mL^{-1}$, the content of ST2 protein in lung homogenate was 47.14 ± 25.43 ng (fig. 2d and e).

Since the hydrodynamic method has been known to cause liver damage, AST and ALT levels were monitored after the injection. In the current study, AST/ALT levels were elevated at day 1, but returned to the normal range by day 2. There were no significant time-course differences in the serum AST/ALT concentration between empty vector-introduced mice and ST2-overexpressing mice (fig. 2f and g).

mRNA expression of pro-inflammatory cytokines, endogenous ST2 and IL-33 in bleomycin-induced lung injury

TNF-α and IL-1β are pro-inflammatory cytokines that have been reported to be upregulated immediately after bleomycin exposure, and to play principal roles in the exacerbation of

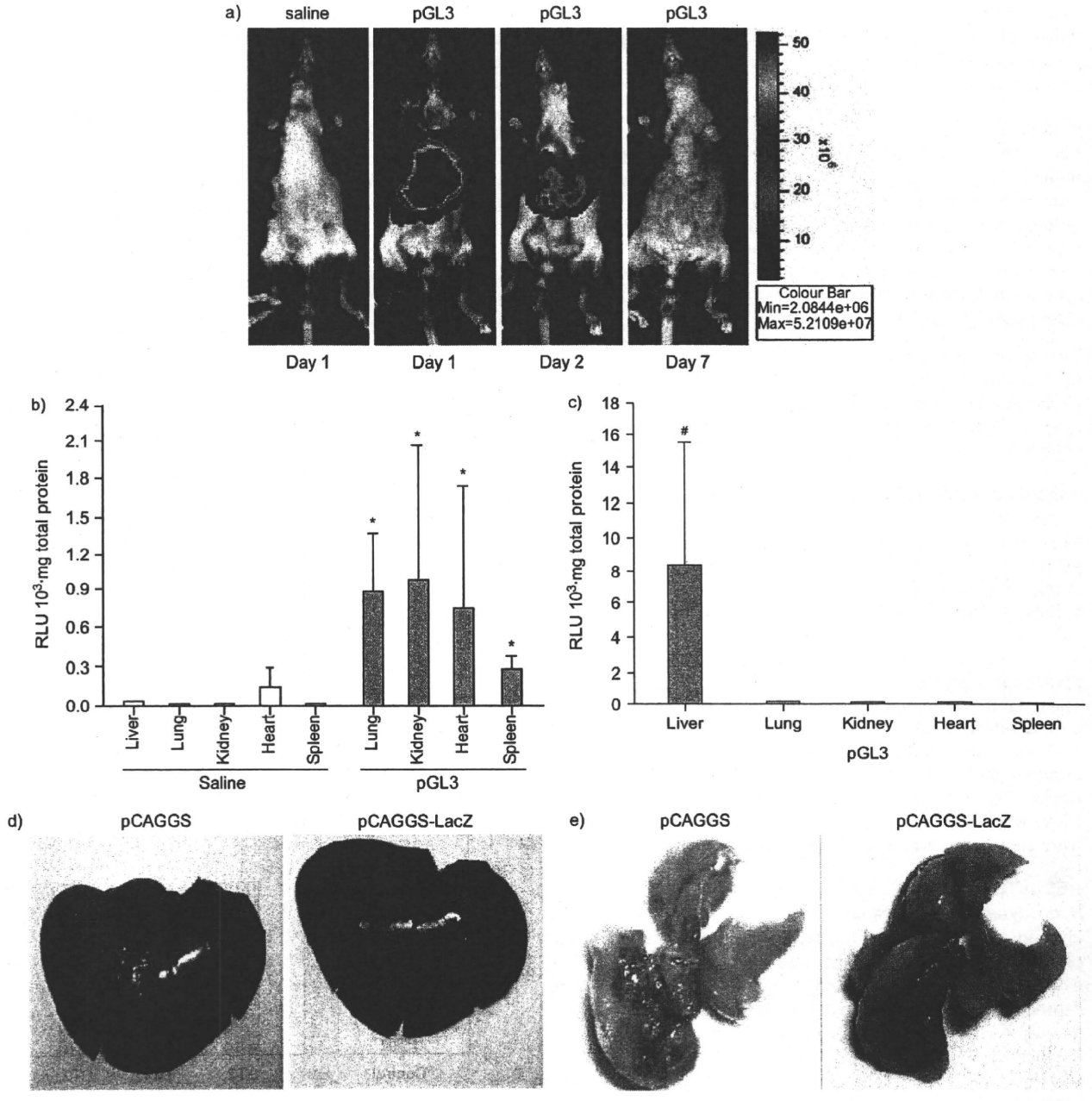

FIGURE 1. Detection of gene expression transferred by hydrodynamic injection. a) *In vivo* imaging of mice after the hydrodynamic injection of saline and pGL3 control vector. Luciferase expression was detected from the ventral surface of the body by IVIS (Xenogen, Alameda, CA, USA) for up to 7 days. The right panel indicates photon intensity correlating with the gene expression. The data are representative of four separate experiments showing similar results. b and c) *Ex vivo* luciferase assay of the individual organs. The luciferase activities of the liver, lung, heart, kidney and spleen at 24 h after the hydrodynamic injection of saline (control; □) and pGL3 control vector (■) were demonstrated as the relative light units (RLU) per total protein content. c) The luciferase activity of the liver was demonstrated independently using another scale. Data are presented as mean±SD, n=4, and are representative of two independent experiments. *: $p<0.05$; **: $p<0.01$ *versus* relevant organ of saline injected group; #: $p<0.01$ *versus* other organs of pGL3-injected mice. General view of the left lobe of the liver (d), and right lobe of the lung (e) at 48 h after the hydrodynamic injection of pCAGGS or pCAGGS-LacZ. Each organ was excised and stained with 5-bromo-4-chloro-3-indolyl-β-D-galactopyranoside solution. Blue staining indicates the expression of β-galactosidase.

lung injury [16, 17]. In the present study, therefore, we examined the lung mRNA expression of the pro-inflammatory cytokines TNF-α and IL-1β after the intratracheal injection of bleomycin. As shown in figure 3, bleomycin treatment remarkably increased the mRNA levels of TNF-α and IL-1β at day 1, demonstrating that acute lung injury occurred. The levels of both cytokines were decreased from day 3–7. We also examined the levels of lung endogenous ST2 and IL-33 mRNA,

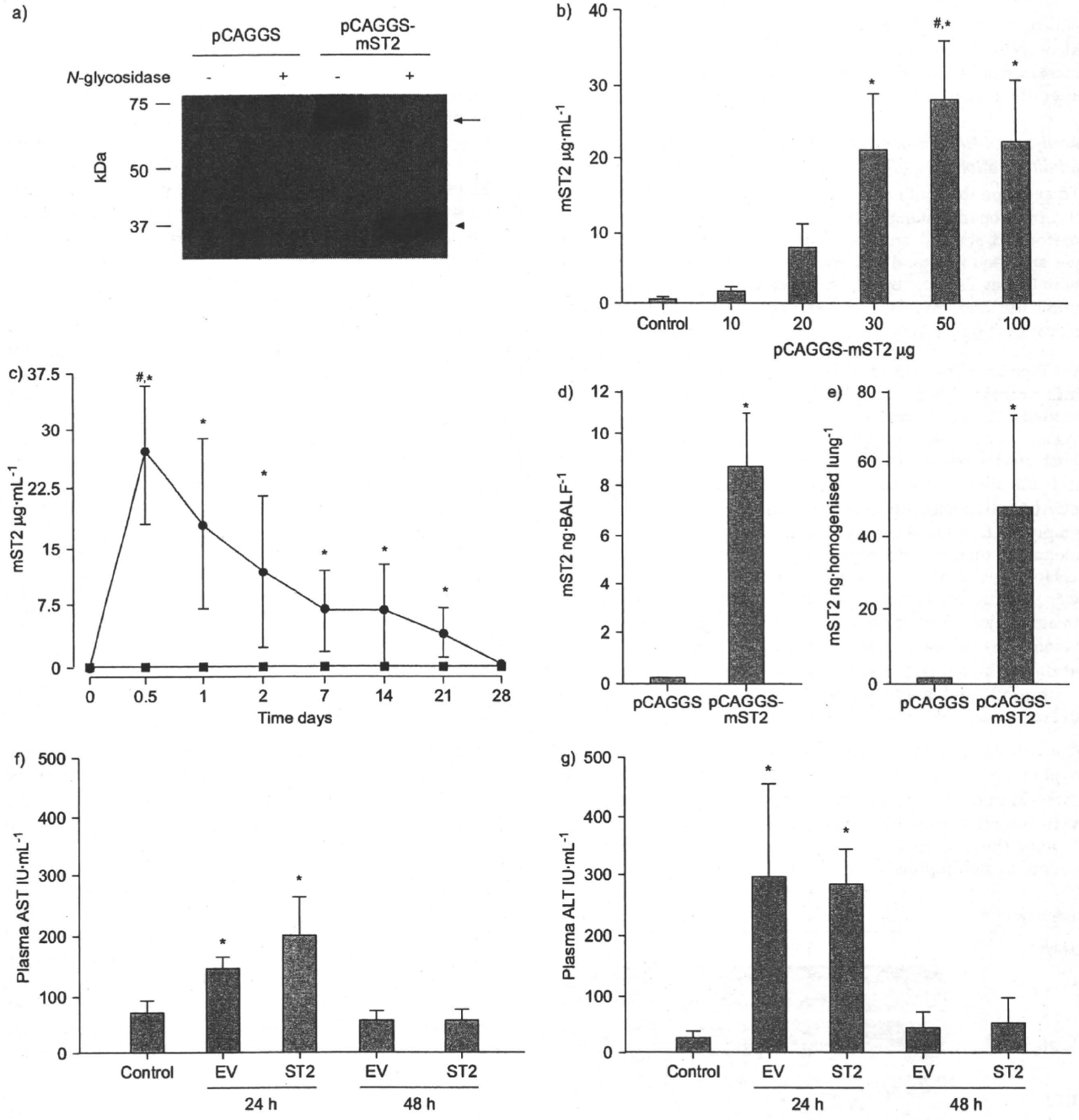

FIGURE 2. Assessment of ST2 gene transfer *in vitro* and *in vivo*. a) *In vitro* detection of mouse ST2 protein in the supernatants of human embryonic kidney (HEK) 293T cells after the gene transfer of pCAGGS and pCAGGS-mST2. These plasmid vectors were transferred by the calcium-phosphate method, and 24 h later, supernatants were collected and subjected to Western blotting. The presence of mature glycosylated ST2 protein (60–70 kDa; arrow) and deglycosylated core peptide (37 kDa; arrowhead) was confirmed. b) Concentration of plasma ST2 protein in mice injected with various amounts of plasmids. Mice were sacrificed at 12 h after the hydrodynamic injection of plasmid (pCAGGS-mST2) or same volume of saline (control), and the plasma was collected to measure the ST2 concentration. The data are presented as mean±SD, n=4, and are representative of three independent experiments. *: $p<0.05$ compared with saline-injected mice; #: $p<0.05$ compared with other plasmid doses. c) Time kinetics of plasma ST2 protein after the hydrodynamic injection with 50 μg of plasmid. Mice were bled consecutively from the tail vein on each day, and plasma was prepared. The data are presented as the mean±SD, n=4, and are representative of three independent experiments. *: $p<0.05$ pCAGGS-injected group *versus* pCAGGS-mST2-injected group at the same plasmid dose; #: $p<0.05$ compared with other timing in pCAGGS-mST2-injected group. ●: pCAGGS-mST2; ■: pCAGGS. d and e) ST2 protein in lung homogenate (d) and bronchoalveolar fluid (BALF; e) at 24 h after hydrodynamic injection. The data are presented as mean±SD, n=3, *: $p<0.05$ compared with pCAGGS-injected mice. f and g) Serum aspartate aminotransferase (AST; f) and alanine aminotransferase (ALT; g) levels after the hydrodynamic gene transfer. The data are presented as the mean±SD, n=3, and are representative of two independent experiments. *: $p<0.05$ compared with saline injected mice (without plasmid injection). EV: empty vector.

which were weakly and constitutively expressed without bleomycin treatment; however, these mRNAs gradually increased in a time-dependent manner from day 3 to day 7 after bleomycin treatment.

Analysis of BALF cell counts and cell types after bleomycin administration

To examine the acute extravasation of inflammatory cells into the pulmonary interstitium caused by bleomycin, BAL was performed at day 1 and day 3 after bleomycin treatment, and we analysed the total cell counts and cell types. Compared with the levels in control mice treated with saline, the total cell numbers and number of neutrophils were significantly elevated at day 1 in bleomycin-treated mice (fig. 4a and b).

We then examined whether the ST2 protein affected the initial inflammatory phase in acute lung injury, using bleomycin-treated ST2-overexpressing mice and mice injected with empty vector as controls. The time course is presented in figure 5. First, it was confirmed that the hydrodynamic injection itself did not affect the total cell count in the empty vector- and pCAGGS-ST2-injected mice (fig. 4a). In mice treated with empty vector plus bleomycin and mice treated with bleomycin alone, the total number of cells immediately increased on day 1. However, in ST2-overexpressing mice, the total cell number was significantly reduced compared with the other bleomycin-treated mice. Furthermore, in mice with empty vector plus bleomycin, numbers of neutrophils were prominently elevated at day 1. In contrast, a significant decrease in the number of neutrophils and lymphocytes was evident on day 1 in ST2-overexpressing mice (fig. 4b).

Conversely, on day 3, the total cell counts in ST2-overexpressing mice were estimated to be almost equivalent to those in mice treated with bleomycin alone, as well as empty vector-injected plus bleomycin-treated mice. However, even though there were no significant statistical differences, the counts of neutrophils were relatively low and the counts of lymphocytes were high in ST2-overexpressing mice, compared with the other bleomycin-treated groups.

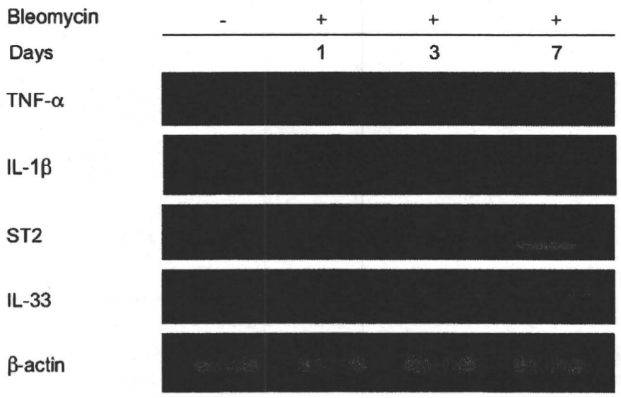

FIGURE 3. mRNA expression of pro-inflammatory cytokines, ST2 and interleukin (IL)-33 after bleomycin treatment. Bleomycin was administered intratracheally to wild-type mice at days 1, 3 and 7, after day 7 the whole lung was excised and each mRNA expression was assayed. Mice without bleomycin treatment were controls. β-actin was a house-keeping gene and provided endogenous control. Similar results were obtained in three separate experiments. TNF-α: tumour necrosis factor-α.

Pro-inflammatory cytokines and albumin levels in BALF

In the present study, total cell counts and neutrophils were particularly increased in the initial phase of bleomycin-induced lung injury. The concentrations of pro-inflammatory cytokines in BALF at day 1 after the bleomycin treatment were then assayed and compared between groups. In bleomycin-treated mice, significant increases of TNF-α, IL-1β (data not shown) and IL-6 were demonstrated, and levels were almost equivalent to or slightly lower than those in the mice treated with empty vector plus bleomycin. In ST2-overexpressing mice, the concentration of TNF-α was significantly reduced compared with that of mice injected with empty vector plus bleomycin or that of mice treated with bleomycin alone (fig. 6a). In addition, the level of IL-6 was also significantly decreased in ST2-overexpressing mice (fig. 6b). The level of IL-1β was slightly lower in ST2-overexpressing mice, but there were no statistically significant differences (data not shown).

The albumin concentration in BALF is frequently used as an indicator of pulmonary vascular permeability, especially in the case of acute lung injury. In fact, bleomycin treatment induced a significant increase in albumin levels in bleomycin-treated mice in the present study. However, in ST2-overexpressing mice, the albumin concentration was significantly lower than in other bleomycin-treated mice (fig. 6c).

Histological examination of the effect of ST2 protein on bleomycin-induced lung injury

The effect of the ST2 protein on acute phases of bleomycin-induced lung injury was investigated histologically (fig. 7a and b). Mice treated only with saline exhibited a small-scale interstitial oedema in the early phase (day 1), but no inflammatory cells were observed in the perivascular area at that time (fig. 7a). The impact of the hydrodynamic injection histologically was also examined; the plasmid injection itself did not affect the pulmonary architecture (fig. 7a). Conversely, both the mice treated with bleomycin alone and those treated with empty vector plus bleomycin showed an accumulation of inflammatory cells around the bronchovascular bundle, and in higher magnification, many neutrophils with segmented nuclei and some round mononuclear cells were recognised (fig. 7b). In contrast, rare inflammatory cells were observed in the peribronchial area in ST2-overexpressing mice, but accumulations of neutrophils were not observed (fig. 7a and b).

In general, following the inflammatory phase in bleomycin-induced lung injury, connective tissues and extracellular matrix are increased [17]. We performed Mallory–Azan and H&E staining of the lung tissue sections on day 7 after administration of bleomycin (fig. 8). Mice treated with saline alone and mice injected with plasmid vector alone had no inflammatory change and no alteration of the pulmonary architecture was observed (fig. 8a). However, a large number of inflammatory cells was observed in the mice treated with bleomycin alone and those treated with empty vector plus bleomycin; the infiltrating cells accumulated in the subpleural and peribronchial areas, and the airspaces showed wide-ranging collapse (fig 8a). Furthermore, there was a large amount of blue-stained connective tissue throughout the alveolar interstitium, especially in the severely

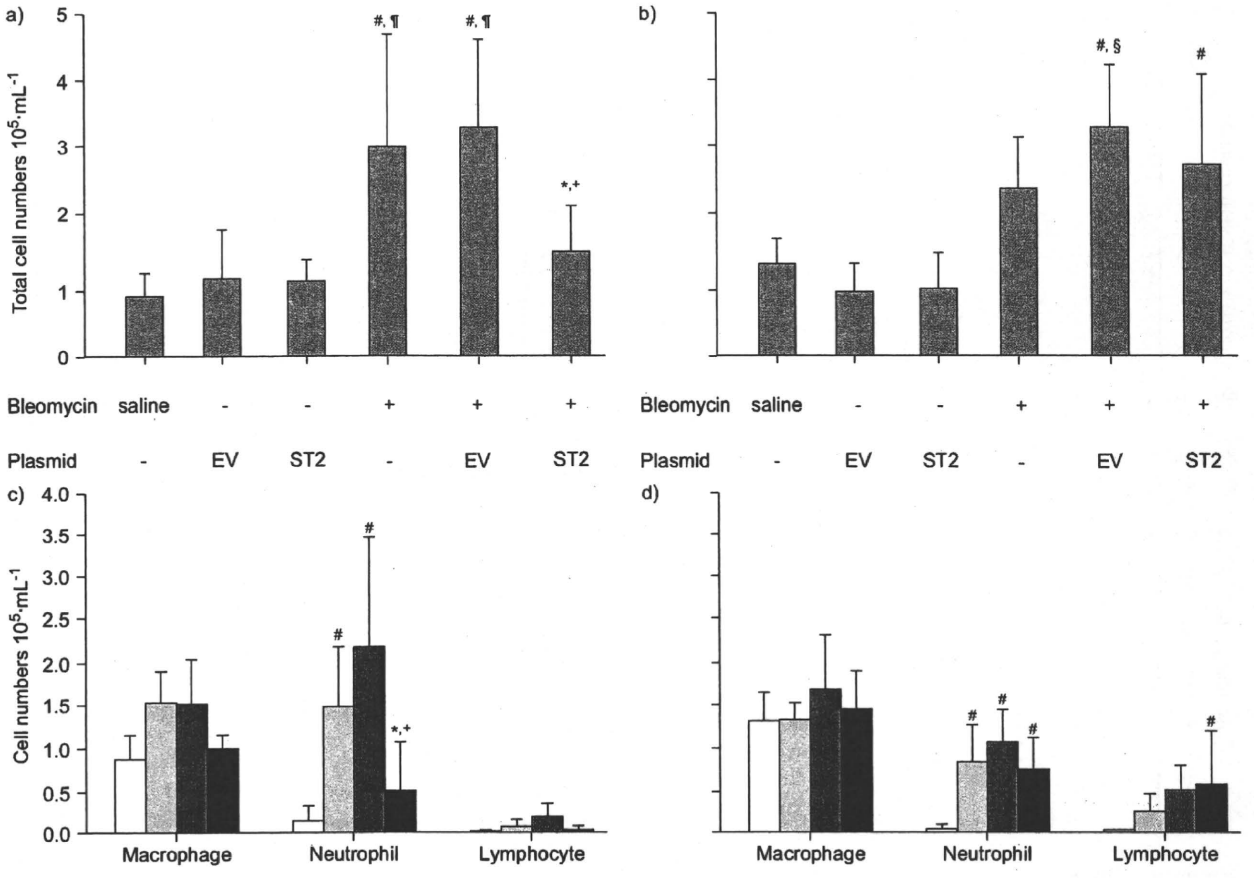

FIGURE 4. Analysis of total cell numbers and cell types in bronchoalveolar lavage fluid (BALF). BALF analysis was performed in mice with or without hydrodynamic gene transfer at day 1 (a and c) and day 3 (b and d) after the administration of bleomycin. a and b) Total cell numbers and c and d) cell types in BALF are shown. The data are presented as the mean±SD of four independent experiments. a and b) Saline: n=5; bleomycin: n=6; EV (empty vector; pCAGGS) or ST2 (pCAGGS-mST2): n=3; and EV or ST2 +bleomycin: n=10 . c and d) Saline (□): n=5; bleomycin (▒): n=6; and EV (■) or ST2+bleomycin (■): n=8. *: $p<0.05$ ST2 plus bleomycin *versus* bleomycin alone; +: $p<0.01$ ST2 plus bleomycin *versus* EV plus bleomycin; #: $p<0.01$ compared with saline; ¶: $p<0.01$ compared with EV and ST2 (without bleomycin); §: $p<0.05$ compared with bleomycin alone.

damaged area (fig. 8b). Conversely, in ST2-overexpressing mice, some inflammatory cells were observed, but the areas of inflammation were restricted. Most of the alveolar structure looked nearly normal, and it was clear that there was less connective tissue compared with other bleomycin-treated mice (fig. 8a and b).

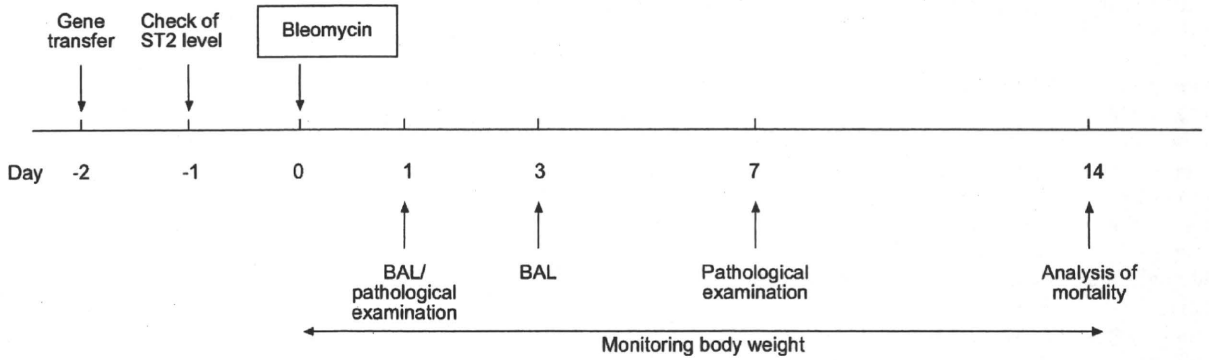

FIGURE 5. Time course of the experiments. The time course of the experiments to examine the effect of ST2 for the bleomycin-induced acute lung injury was presented schematically. The gene transfer was performed by the hydrodynamic injection of plasmids. BAL: bronchoalveolar lavage.

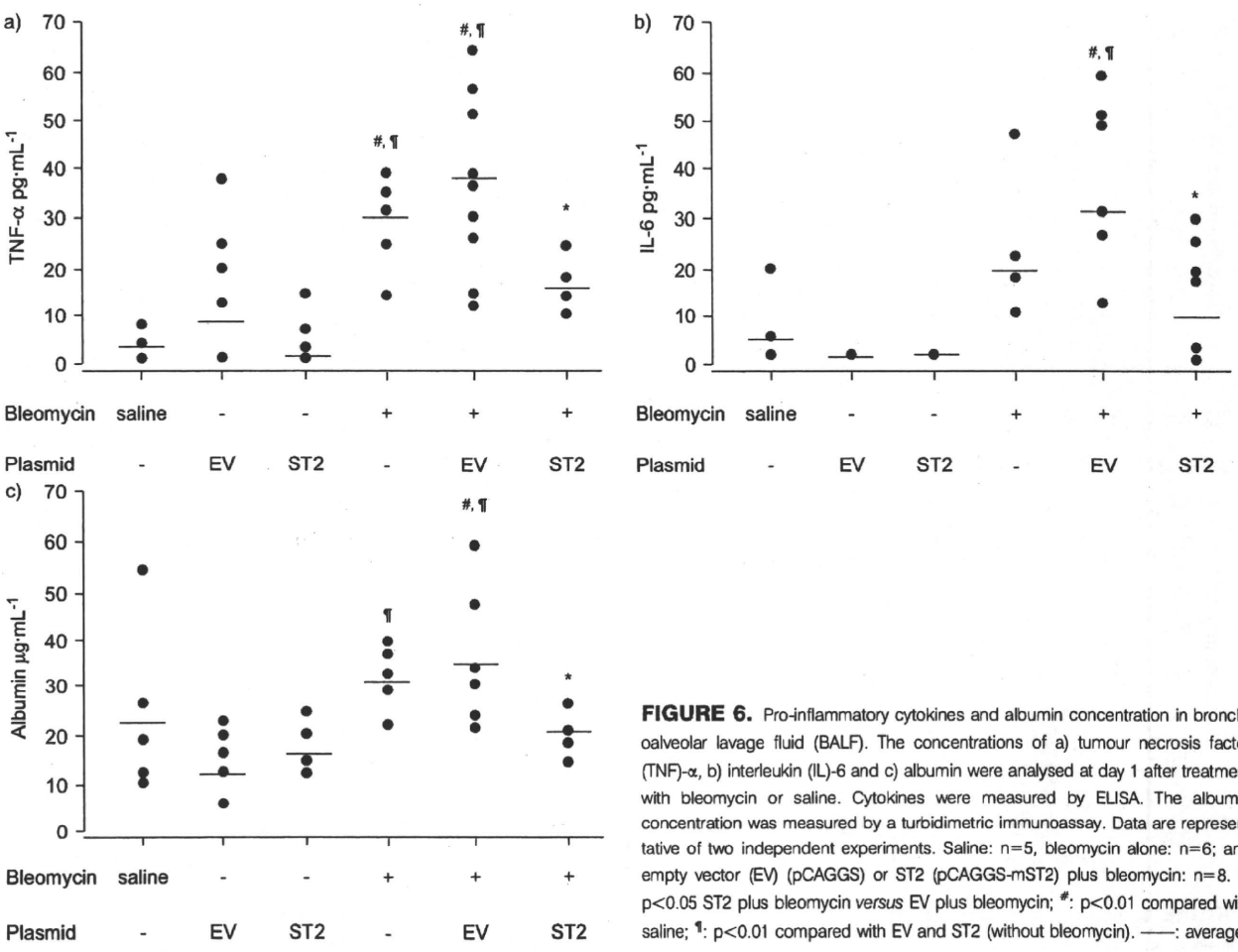

FIGURE 6. Pro-inflammatory cytokines and albumin concentration in bronchoalveolar lavage fluid (BALF). The concentrations of a) tumour necrosis factor (TNF)-α, b) interleukin (IL)-6 and c) albumin were analysed at day 1 after treatment with bleomycin or saline. Cytokines were measured by ELISA. The albumin concentration was measured by a turbidimetric immunoassay. Data are representative of two independent experiments. Saline: n=5, bleomycin alone: n=6; and empty vector (EV) (pCAGGS) or ST2 (pCAGGS-mST2) plus bleomycin: n=8. *: $p<0.05$ ST2 plus bleomycin *versus* EV plus bleomycin; #: $p<0.01$ compared with saline; ¶: $p<0.01$ compared with EV and ST2 (without bleomycin). ——: average.

Next, Scion Image software was used (Scion Corporation, Frederick, MD, USA) to quantify TVD to visualise the histological results at day 7 after bleomycin treatment. TVD was presented as the ratio of the collapsed high-density area to total area, and it increased in proportion to the extent of lung injury. Mice treated with bleomycin alone or treated with empty vector plus bleomycin showed significantly higher TVD than saline-treated mice. Conversely, in ST2-overexpressing mice treated with bleomycin, TVD was significantly lower than in other bleomycin-treated mice (fig. 8c).

Body weight loss and survival rate in bleomycin-induced lung injury

Body weight loss was monitored during the 14 days after bleomycin administration in ST2-overexpressing mice and empty vector-injected mice (fig. 9a). During the first week, most of the experimental mice remained alive, but their body weights decreased to varying degrees. In the second week, although the difference between the two groups was not statistically significant, the empty vector-injected mice continuously lost body weight, while the body weight of the ST2-overexpressing mice tended to remain constant.

Finally, we compared the survival rate for 14 days after bleomycin administration between ST2-overexpressing mice and the other groups of mice (saline, bleomycin and empty vector plus bleomycin; fig. 9b). The survival rate of ST2-overexpressing mice was 84.0% at day 14 and the mean survival time was 13.44 days (95% confidence interval (CI) 12.92–13.96). The survival rates of mice treated with an empty vector plus bleomycin and bleomycin treatment alone were 43.5% and 63.6% and mean survival times were 11.7 (95% CI 10.58–12.81) and 12.2 days and (95% CI 10.76–13.60), respectively. ST2-overexpressing mice showed significantly higher survival rates than the other control groups. No mice died from hydrodynamic injection only (data not shown).

DISCUSSION

Some recent reports have suggested that the ST2 protein is induced by various inflammatory stimuli and may play an anti-inflammatory role *in vivo* [6–10]. TAJIMA and co-workers [8, 18] reported an increase of serum ST2 protein in acute exacerbation of idiopathic pulmonary fibrosis, and that ST2 gene expression was induced in the murine lung by intratracheal administration of bleomycin. Therefore, we speculated that ST2 was closely related to lung inflammation. We induced acute lung injury using bleomycin in the present study, and then assessed the effect of ST2 protein *in vivo*.

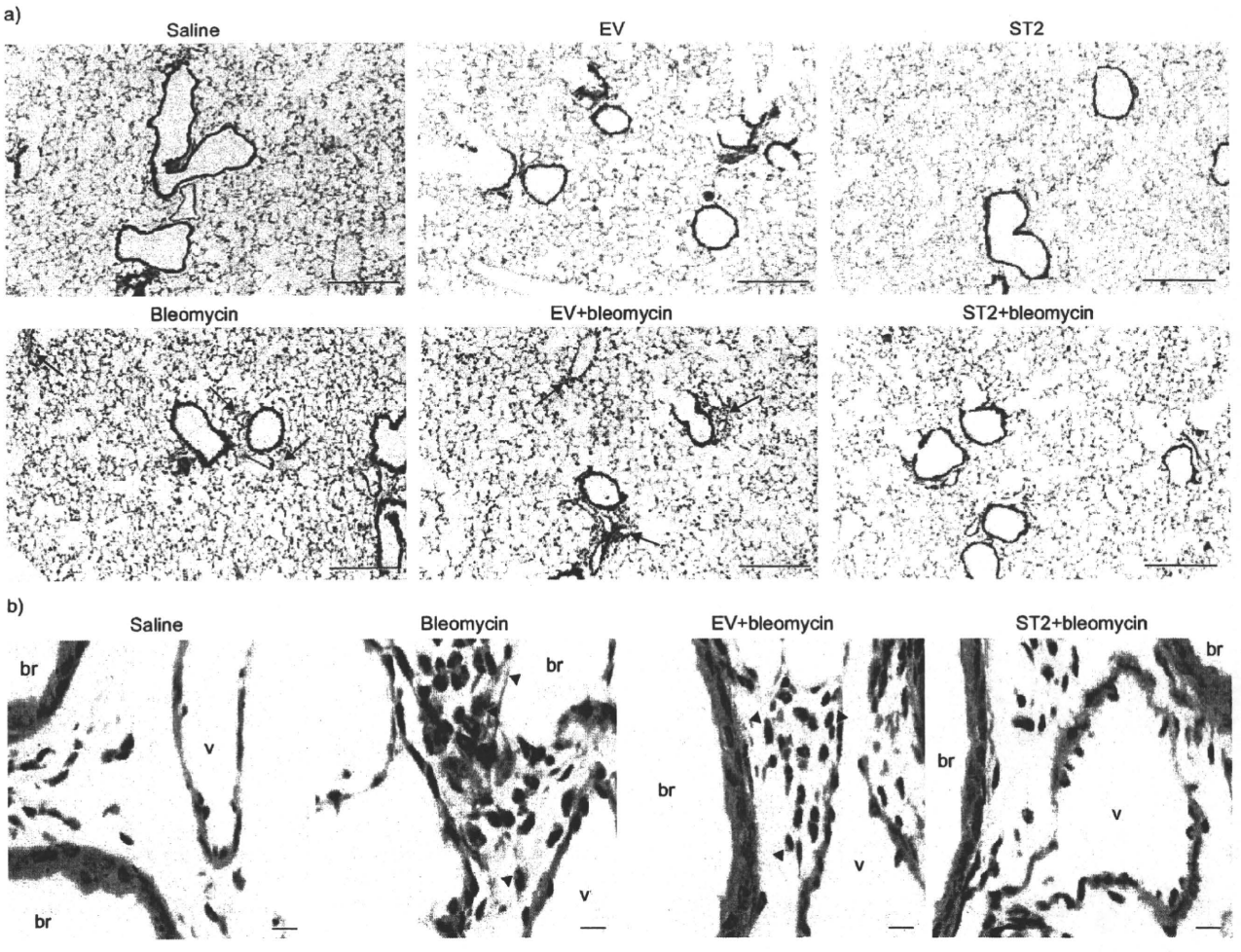

FIGURE 7. Histological findings at day 1 after treatment with bleomycin. Photomicrographs of lung sections from mice treated with saline, empty vector (EV; pCAGGS) alone, ST2 (pCAGGS-mST2) alone, bleomycin alone, EV plus bleomycin and ST2 plus bleomycin at day 1 after treatment. a) Lower magnification (Scale bars=200 μm) and b) focused on bronchovascular bundles at a higher magnification (Scale bars=10 μm) of mice treated with saline, bleomycin alone, EV plus bleomycin and ST2 plus bleomycin. Sections were stained with haematoxylin and eosin. Arrows: accumulation of inflammatory cells; arrowheads: neutrophils. br: bronchiole; v: vessel.

In order to examine the effect of the ST2 protein in mice, we first purified and administered recombinant ST2 protein to mice. However, unlike *in vitro* studies, an enormous amount of ST2 protein was needed in order to attain the high ST2 level *in vivo*. Then, a hydrodynamic injection method was employed, which is an efficient method for transient gene transfer to adult animals [13, 14, 19], and high levels of target gene expression can be achieved by the rapid injection of naked plasmid in a large volume. Corroborating previous reports [19], we confirmed that the main transgene-expressing organ was the liver; however, the ST2 protein was released into the systemic circulation and attained a high level 12 h after the gene transfer. The transgene expression level depends on the injection speed, injection volume, target organ and the choice of promoter of the plasmid vectors. We used the pCAGGS vector, which was driven by the chicken β-actin promoter that enabled us to maintain a high level of expression in mammalian cells. However, the appropriate plasma ST2 level to achieve an anti-inflammatory effect for mice treated with bleomycin has not been established *in vivo*. According to a previous report, 100 μg of ST2 protein is required to prevent endotoxin shock in mice [9]. Therefore, in the present study, we used a high dose of plasmid (50 $\mu g \cdot mouse^{-1}$) to obtain the maximal plasma concentration of ST2 (18.1–27.6 $\mu g \cdot mL^{-1}$).

In the present report, we demonstrated that the ST2 protein hindered the invasion of neutrophils and the subsequent capillary leakage in acute lung injury for the first time. In addition, TNF-α, IL-1β and IL-6 are known to play pivotal roles in the induction of lung inflammation, leukocyte migration, and the production of other cytokines and chemokines [20, 21], and these cytokines were elevated in BALF in bleomycin-induced acute lung injury. However, we found that the levels of TNF-α and IL-6 in BALF were significantly decreased in ST2-overexpressing mice at day 1 after bleomycin treatment. In previous *in vitro* experiments, it was demonstrated that ST2 inhibited the production of pro-inflammatory cytokines in macrophages derived from bone marrow [9, 11], as well as in a

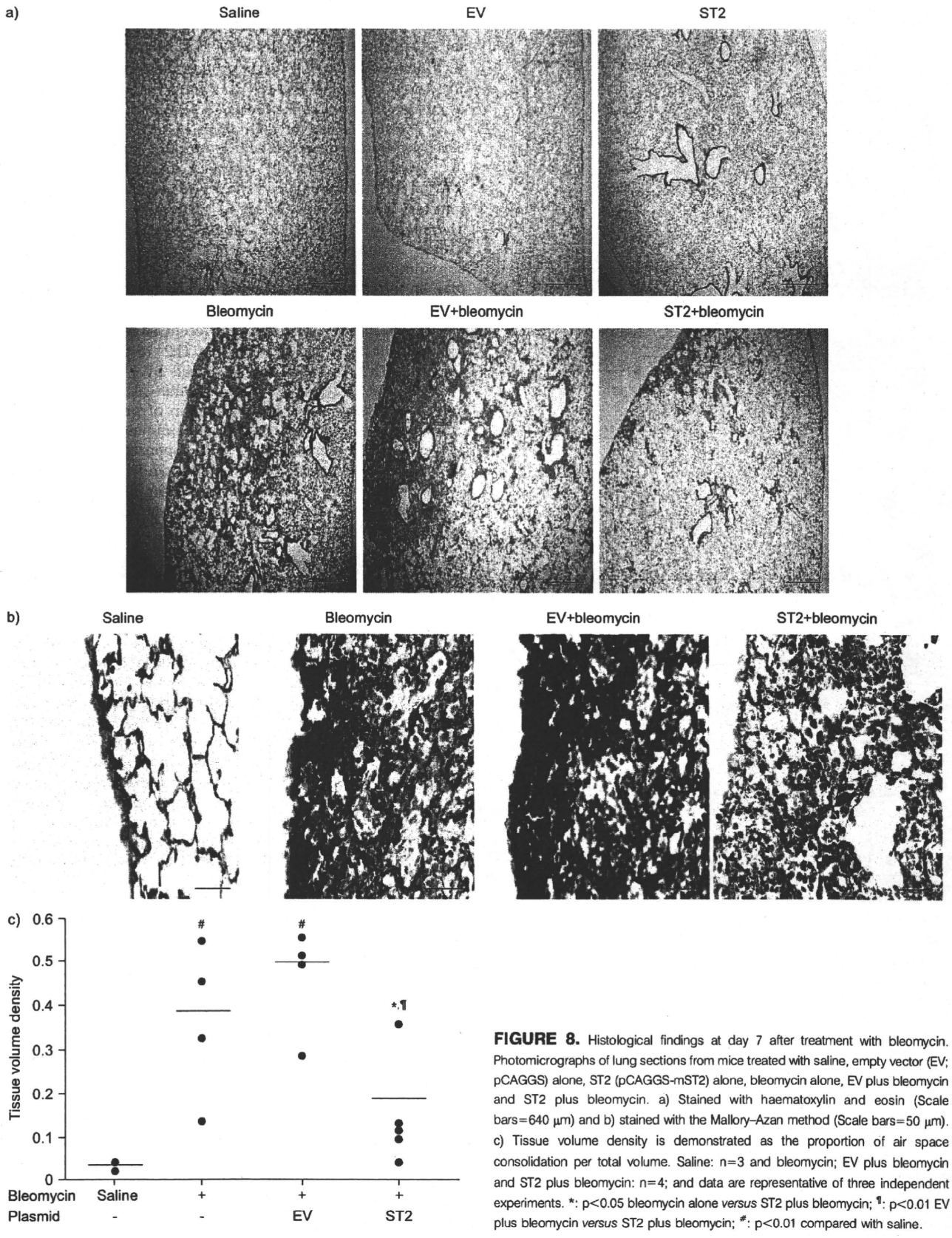

FIGURE 8. Histological findings at day 7 after treatment with bleomycin. Photomicrographs of lung sections from mice treated with saline, empty vector (EV; pCAGGS) alone, ST2 (pCAGGS-mST2) alone, bleomycin alone, EV plus bleomycin and ST2 plus bleomycin. a) Stained with haematoxylin and eosin (Scale bars=640 μm) and b) stained with the Mallory–Azan method (Scale bars=50 μm). c) Tissue volume density is demonstrated as the proportion of air space consolidation per total volume. Saline: n=3 and bleomycin; EV plus bleomycin and ST2 plus bleomycin: n=4; and data are representative of three independent experiments. *: $p<0.05$ bleomycin alone *versus* ST2 plus bleomycin; ¶: $p<0.01$ EV plus bleomycin *versus* ST2 plus bleomycin; #: $p<0.01$ compared with saline.

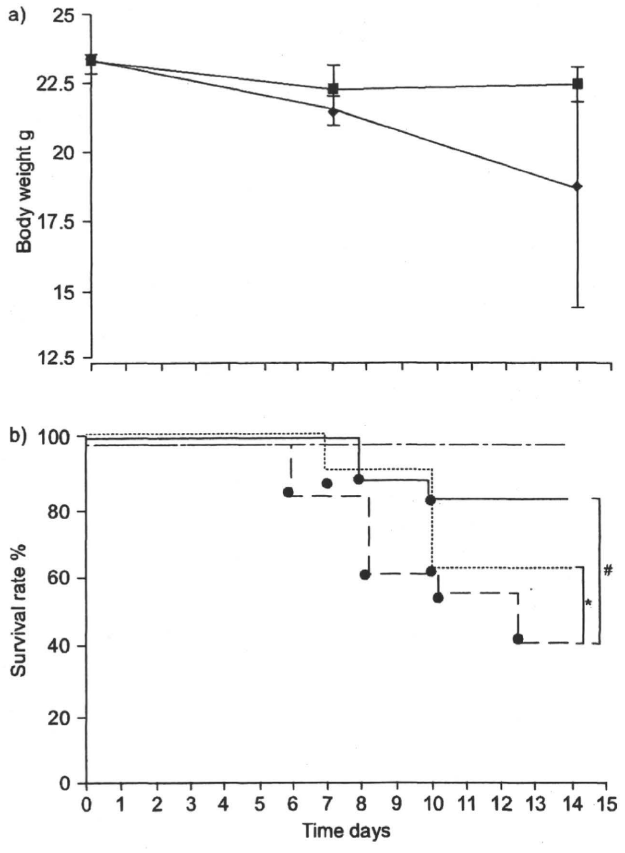

FIGURE 9. Body weight loss and survival rate of mice with bleomycin-induced lung injury. a) Comparison of body weight loss in mice treated with empty vector (EV) plus bleomycin (◆) and ST2 (pCAGGS-mST2) plus bleomycin (■) between day 0–14 (n=8 in both groups); p=0.08. b) The survival rate of mice was monitored for 14 days and analysed using the Kaplan–Meier method. Mice that died through injurious tracheotomy or deep anaesthesia were excluded. Saline (– · – · –): n=7; bleomycin alone (· · · ·): n=14; and EV plus bleomycin (- - - -) or ST2 plus bleomycin (——): n=23. *: $p<0.05$ bleomycin alone *versus* ST2 plus bleomycin; #: $p<0.01$ EV plus bleomycin *versus* ST2 plus bleomycin (see online supplementary material). Serum ST2 level after the injection of lipopolysaccharide (LPS) at 7.5 mg·kg^{-1} intravenously. This model mimicked human septic shock. The concentration of serum ST2 was examined using the mouse ST2 ELISA system. Serum ST2 were markedly elevated 12–24 h after LPS injection and rapidly declined at 48 h.

monocytic leukaemia cell line [10]. Therefore, in the present *in vivo* models, we speculated that overexpressed plasma ST2 infiltrated the alveolar spaces, where it affected alveolar macrophages to suppress the production of cytokines, and subsequently suppressed the migration of neutrophils and increased vascular permeability.

In contrast, we did not detect any significant differences in BALF findings from day 3 after bleomycin treatment. It was speculated that the following aetiological explanations might account for the BALF findings from day 3: 1) ST2 could play an anti-inflammatory role only during the initial phase of the acute lung injury, and thus, could not stop the infiltration of inflammatory cells after 3 days; 2) ST2 overexpression in this system peaked at 12–24 h after gene transfer, and then ST2 rapidly declined (thus, the effects of ST2 would diminish along with attenuation of the plasma concentration of ST2); and 3) ST2 could cause adverse effects from day 3 after bleomycin treatment. In association with the second point, hydrodynamic gene transfer is certainly an invasive approach; and thus, repetitive transfer was difficult in our pilot study, because the mice were often dead by repeated injection. Therefore, a method for maintaining high ST2 levels even after 48 h of gene transfer must be developed to assess the effects of ST2 accurately in this model. In association with the third point, it was reported that serum ST2 was elevated in some autoimmune diseases [22], and ST2L has been reported to play an important role in the differentiation of T-helper (Th) cells, which induce the proliferation and activation of Th2 response [22, 23]. Furthermore, a recent study reported that recombinant ST2 boosted hepatic Th2 responses *in vivo*, increased Th2 cytokines and advanced liver fibrosis [24]. It suggests that ST2 protein plays an ambivalent dual role as follows: ST2 suppresses the production of pro-inflammatory cytokines from macrophages (anti-inflammatory effect), and conversely, ST2 stimulates the Th2 response (pro-inflammatory effect). Considering these reports, we hypothesised that overexpresssed-ST2 protein may affect lymphocyte proliferation in this model, which would cause the adverse effects from the increase of total cells seen after day 3.

We found that endogenous ST2 mRNA and IL-33 were concurrently increased at day 3 after bleomycin treatment, whereas pro-inflammatory cytokines (TNF-α and IL-1β) were increased immediately after bleomycin treatment. The effects of ST2 and IL-33 have been well investigated in allergic diseases; IL-33 is known to strongly induce the production of Th2 cytokines and IgE and increase the proliferation of eosinophils [6, 25]. TAJIMA *et al.* [8] reported that endogenous ST2 and Th2 cytokines (IL-4, IL-5) were slowly induced after bleomycin-treatment, similarly to our study. From these results, endogenous ST2, Th2 cytokines and IL-33 would affect the progress of lung injury following the initial phase of acute lung injury. It is thought to be important whether overexpressed-ST2 affects IL-33 production; however, we could not approach that problem because of the difficulty of keeping the high level of ST2 at day 3 after bleomycin treatment.

From day 7 after bleomycin treatment, pulmonary remodelling progressed, and we found subpleural collapse and an increase of collagen fibres rather than peribronchial accumulation of inflammatory cells. Around half of the bleomycin-treated mice and half of the mice treated with empty vector plus bleomycin died during days 7–14, suggesting that the pulmonary remodelling phase (days 7–14) was most responsible for mortality. In ST2-overexpressing mice, the histological findings and survival rate after bleomycin treatment were improved compared with other bleomycin-treated mice. Pulmonary remodelling was mostly caused by the degradation of extracellular matrix by neutrophils [26] and the initial increase of neutrophils plays a critical role in the progress of lung inflammation and fibrosis [27]. Considering the previous reports and our present data, we found that inhibiting the infiltration of neutrophils by ST2 at an early stage of lung

injury helped to protect against proteolysis, minimised histological change and improved survival rates, even though the peribronchial inflammation, as indicated by the BALF findings, could not be completely suppressed.

In order to conclusively determine the roles of ST2, it will be necessary to conduct similar experiments using ST2 knockout (KO) mice. Although several studies using ST2 KO mice have been reported, unfortunately both specific soluble ST2 and transmembrane ST2L were absent in these mice, because the disrupted DNA of KO mice corresponds to a common portion of ST2 and ST2L [28]. Therefore, utilising available KO mice for the study of the involvement of ST2 in the lung inflammation would complicate the outcome. However, we speculate that previous results and the findings of the current study suggest that bleomycin would cause serious damage to the ST2-specific KO mice.

In conclusion, the present study confirmed that ST2 possesses the ability to suppress lung inflammation by inhibiting the elevation of pro-inflammatory cytokine levels and the accumulation of neutrophils, and by reducing vascular permeability. Further investigation into the aetiology of the effects of ST2 is required before the clinical applications are confirmed. However, ST2 could be a new candidate for the treatment of lethal acute lung injury.

ACKNOWLEDGEMENTS

The current authors would like to thank J. Miyazaki (Osaka University, Osaka, Japan) and T. Murakami (Jichi Medical Unfiversity, Tochigi, Japan) for providing plasmids and T. Kasahara (Kyoritsu College of Pharmacy, Tokyo, Japan) for providing HEK293T cells. We also thank R. Izawa and M. Mato for excellent technical support, and K. Kishi (all Jichi Medical University) for advice on statistical analysis. N. Mato (Jichi Medical University) thanks Jichi Medical University for awarding this research the Young Investigator Award.

REFERENCES

1 Bedrossian CW. Iatrogenic and toxic injury. *In*: Dail DH, Hammar SP, eds. Pulmonary Pathology. New York, Springer-Verlag, 1988; pp. 511–517.
2 Ware LB, Matthay MA. The acute respiratory syndrome. *N Engl J Med* 2000; 342: 1334–1349.
3 Tominaga S. A putative protein of a growth specific cDNA from BALB/c-3T3 cells is highly similar to the extracellular portion of mouse interleukin 1 receptor. *FEBS Lett* 1989; 258: 301–304.
4 Tominaga S, Kuroiwa K, Tago K, *et al.* Presence of expression of novel variant form of ST2 gene product in human leukemic cell line UT-7/GM. *Biochem Biophys Res Commun* 1999; 264: 14–18.
5 Schmitz J, Owyang A, Oldham E, *et al.* IL-33, an interleukin-1-like cytokine that signals *via* the IL-1 receptor-related protein ST2 and induces T helper type 2-associated cytokines. *Immunity* 2005; 23: 479–490.
6 Brunner M, Krenn C, Roth G, *et al.* Increased levels of soluble ST2 protein and IgG1 production in patients with sepsis and trauma. *Intensive Care Med* 2004; 30: 1468–1473.
7 Oshikawa K, Yanagisawa K, Tominaga S, *et al.* ST2 protein induced by inflammatory stimuli can modulate acute lung inflammation. *Biochem Biophys Res Commun* 2002; 299: 18–24.
8 Tajima S, Oshikawa K, Tominaga S, *et al.* The increase in serum soluble ST2 protein upon acute exacerbation of idiopathic pulmonary fibrosis. *Chest* 2003; 124: 1206–1214.
9 Sweet MJ, Leung BP, Kang D, *et al.* A novel pathway regulating lipopolysaccharide-induced shock by ST2/T1 *via* inhibition of Toll-like receptor 4 expression. *J Immunol* 2001; 166: 6633–6639.
10 Takezako N, Hayakawa M, Hayakawa H, *et al.* ST2 suppresses IL-6 production *via* the inhibition of IκB degradation induced by the LPS signal in THP-1 cells. *Biochem Biophys Res Commun* 2006; 341: 425–432.
11 Leung BP, Xu D, Culshaw S, *et al.* A novel therapy of murine collagen-induced arthritis with soluble T1/ST2. *J Immunol* 2004; 173: 145–150.
12 Takagi T, Yanagisawa K, Tsukamoto T, *et al.* Identification of the product of the murine ST2 gene. *Biochim Biophys Acta* 1993; 1178: 194–200.
13 Inoue S, Hakamata Y, Kaneko M, *et al.* Gene therapy for organ grafts using rapid injection of naked DNA: application to the rat liver. *Transplantation* 2004; 77: 997–1003.
14 Hakamata Y, Murakami T, Kobayashi E. "Firefly rats" as an organ/cellular source for long-term *in vivo* bioluminescent imaging. *Transplantation* 2006; 81: 1179–1184.
15 Howell DC, Johns RH, Lasky JA, *et al.* Absence of proteinase-activated receptor-1 signaling affords protection from bleomycin-induced lung inflammation and fibrosis. *Am J Pathol* 2005; 166: 1353–1365.
16 Kelley J, Newman RA, Evans JN. Bleomycin-induced pulmonary fibrosis in the rat. Prevention with an inhibitor of collagen synthesis. *J Lab Clin Med* 1980; 96: 954–964.
17 Lindenschmidt RC, Tryka AF, Godfrey GA, *et al.* Intratracheal *versus* intravenous administration of bleomycin in mice: acute effects. *Toxicol Appl Pharmacol* 1986; 85: 69–77.
18 Tajima S, Bando M, Ohno S, *et al.* ST2 gene induced by type 2 helper T cell (Th2) and proinflammatory cytokine stimuli may modulate lung injury and fibrosis. *Exp Lung Res* 2007; 33: 81–97.
19 Zhang G, Budker V, Wolff JA. High levels of foreign gene expression in hepatocytes after tail vein injections of naked plasmid DNA. *Hum Gene Ther* 1999; 10: 1735–1737.
20 Piguet PF, Collart MA, Grau GE, *et al.* Tumor necrosis factor/cachectin plays a key role in bleomycin-induced pneumopathy and fibrosis. *J Exp Med* 1989; 170: 655–663.
21 Jordana M, Richards C, Irving LB, *et al.* Spontaneous *in vitro* release of alveolar-macrophage cytokines after the intratracheal instillation of bleomycin in rats. Characterization and kinetic studies. *Am Rev Respir Dis* 1988; 137: 1135–1140.
22 Kuroiwa K, Arai T, Okazaki H, *et al.* Identification of human ST2 protein in the sera of patients with autoimmune diseases. *Biochem Biophys Res Commun* 2001; 284: 1104–1108.
23 Trajkovic V, Sweet MT, Xu D. T1/ST2 – an IL-1 receptor-like modulator of immune responses. *Cytokine Growth Factor Rev* 2004; 15: 87–95.
24 Amatucci A, Novobrantseva T, Gilbride K, *et al.* Recombinant ST2 boosts hepatic Th2 response *in vivo*. *J Leukoc Biol* 2007; 82: 124–132.

25 Kurowska-Stolarska M, Kewin P, Murphy G, *et al.* IL-33 induces antigen-specific IL-5+ T cells and promotes allergic-induced airway inflammation independent of IL-4. *J Immunol* 2008; 181: 4780–4790.

26 Dunsmore SE, Roes J, Chua FJ, *et al.* Evidence that neutrophil elastase-deficient mice are resistant to bleomycin-induced fibrosis. *Chest* 2001; 120: 35S–36S.

27 Gasse P, Mary C, Guenon I, *et al.* IL-1R1/MyD88 signaling and the inflammasome are essential in pulmonary inflammation and fibrosis in mice. *J Clin Invest* 2007; 117: 3786–3799.

28 Townsend MJ, Fallon PG, Matthews DJ, *et al.* T1/ST2-deficient mice demonstrate the importance of T1/ST2 in developing primary T helper cell type 2 responses. *J Exp Med* 2000; 191: 1069–1076.

Lung (2009) 187:331–339
DOI 10.1007/s00408-009-9162-6

INTERSTITIAL LUNG DISEASE

Effects of IS-741, a Synthetic Anti-Inflammatory Agent, on Bleomycin-Induced Lung Injury in Mice

Yuichi Shimaoka · Shunji Tajima · Fumio Fujimori · Cristiane Yamabayashi · Hiroshi Moriyama · Masaki Terada · Toshinori Takada · Eiichi Suzuki · Masashi Bando · Yukihiko Sugiyama · Ichiei Narita

Received: 3 April 2009 / Accepted: 21 July 2009 / Published online: 13 August 2009

Abstract Bleomycin (BLM)-induced lung injury consists of excessive inflammatory cell infiltration and fibrosis. IS-741 has been reported to be an anti-inflammatory drug through an inhibitory action on cell adhesion. In this study we investigated whether IS-741 could inhibit the progression of pulmonary fibrosis through inflammatory cell infiltration. Lung injury was induced in female C57BL/6 mice by intratracheal instillation of BLM. IS-741 was administered daily intraperitoneally. The hydroxyproline content and fluid content in the lung on Day 28 were significantly lower in the IS-741-treated mice. The histological degree of lung injury or fibrosis was reduced in IS-741-treated mice. Administration of IS-741 caused significant reduction in the absolute number of total cells, monocyte chemoattractant protein (MCP)-1, and cysteinyl leukotriene (cysLTs) levels in bronchoalveolar lavage fluid on Day 7. Furthermore, the hydroxyproline content was significantly lower in IS-741-treated mice even though IS-741 was started on Day 14 after BLM instillation. Treatment with IS-741 had an inhibitory effect on BLM-induced lung injury and fibrosis via the repression of MCP-1 or cysLTs in this murine experimental model.

Y. Shimaoka · S. Tajima (✉) · F. Fujimori · C. Yamabayashi · H. Moriyama · M. Terada · T. Takada · E. Suzuki · I. Narita
Division of Respiratory Medicine, Graduate School of Medical and Dental Sciences, Niigata University, 1-757 Asahimachi-dori, Chuo-ku, Niigata 951-8510, Japan
e-mail: tajimash@med.niigata-u.ac.jp

M. Bando · Y. Sugiyama
Division of Pulmonary Medicine, Department of Medicine, Jichi Medical University, 3311-1 Yakushiji, Shimotsuke, Tochigi 329-0498, Japan

Keywords Bleomycin · IS-741 · Lung injury · Monocyte chemoattractant protein-1 · Pulmonary fibrosis · Cysteinyl leukotrienes

Introduction

It is generally accepted that fibrosis is not a mere end-product of chronic injury, but an active, dynamic process that may be reversible in the early stage of the injury. Moreover, it is supposed that accumulation of leukocytes in the inflamed site and their subsequent interaction with resident fibroblasts might be important in various forms of organic fibrosis [1–5]. Idiopathic pulmonary fibrosis (IPF) is defined as a specific form of chronic fibrosing interstitial pneumonia limited to the lung [6]. The etiology of IPF is not known and it remains a devastating disease with a more than 50% 5-year mortality rate [6]. Unfortunately, the pathogenesis of IPF is also incompletely understood. Although several drugs have been used or tried for treating IPF, there is no established treatment that definitely improves its outcome [6]. Thus, we await new therapies based on a new understanding of the pathogenesis of IPF.

The *N*-(2-ethylsulfonyl-amino-5-trifluoromethyl-3-pyridinyl) carboxamide derivative IS-741 is reported to have an inhibitory effect on cytosolic phospholipase A_2 ($cPLA_2$) and attenuates experimental acute pancreatitis in dogs [7, 8]. IS-741 was also shown to inhibit the expression of macrophage antigen (Mac)-1 (CD11b/CD18) or lymphocyte function-associated antigen (LFA)-1 (CD11a/CD18), a cell adhesion molecule on the surface of circulating neutrophils, and block the adhesion between inflammatory cells and microvascular endothelial cells in vivo and in vitro [9, 10]. In previous studies it was demonstrated that treatment with IS-741 significantly attenuated inflammation in

various inflammatory experimental models such as acute pancreatitis [10–12], ileitis [13], and colitis [9, 14]. The mechanism by which IS-741 prevents the development of acute pancreatitis and colitis might be its inhibitory effect on the adhesion of neutrophils to endothelial cells and subsequent neutrophil infiltration into the pancreatic tissue or intestinal mucosa of the colon. Recently, Kaku et al. [15] have shown that IS-741 attenuates local migration of monocytes and subsequent pancreatic fibrosis via decreased mRNA expressions of monocyte chemoattractant protein (MCP)-1 and LFA-1 in experimental chronic pancreatitis induced by dibutyltin dichloride in rats. Although there are some publications about the effect of IS-741 on the various inflammatory or fibrotic experimental models as above, there are no reports on the effect of IS-741 on the bleomycin (BLM)-induced pulmonary fibrosis model.

Thus, in the present study the established model of BLM-induced lung injury in mice was used to investigate IS-741's inhibition of BLM-induced inflammation and fibrosis.

Materials and Methods

Mice and Reagents

All mice received humane care in accordance with the Guide for the Care and Use of Laboratory Animals, published by the US National Institutes of Health (NIH publication 8523, revised 1985; http://www.nyu.edu/uawc/Forms/Guide-excerpts.pdf). The study protocol was approved by the Ethics Committee for animal experiments of Niigata University, Niigata, Japan. Specific pathogen-free female C57BL/6 mice, 6–8 weeks of age, were obtained from Japan SLC (Niigata, Japan) and housed in the animal facility of Niigata University. BLM was purchased from Nippon Kayaku (Tokyo, Japan). IS-741 was kindly supplied by Ishihara Sangyo Ltd (Osaka, Japan). IS-741 in 1 ml of normal saline was administered intraperitoneally to the mice at a dose of 10 mg/kg/day.

BLM-Induced Pulmonary Fibrosis Model

We used C57BL/6 mice because they are a well-characterized inbred strain that is susceptible to BLM-induced lung injury. To induce pulmonary fibrosis, we treated C57BL/6 mice with intratracheal BLM on Day 0. The C57BL/6 mice were anesthetized by the intraperitoneal administration of 0.01 ml/g 10% pentobarbital sodium solution (Abbott Laboratories, North Chicago, IL, USA), followed by intratracheal instillation of 3 mg BLM/kg body weight in 50 μl of sterile isotonic saline. The control animals received intratracheal saline only.

The mice were randomly divided into six study groups as shown in Fig. 1: (A) the BLM group received normal saline intraperitoneally and intratracheal BLM injection; (B) the BLM + IS-741 group received IS-741 intraperitoneally for 5 weeks and intratracheal BLM injection; (C) the IS-741 group received IS-741 intraperitoneally and intratracheal saline injection; (D) the Control group received normal saline for 5 weeks and saline instillation; (E) the BLM + IS-741 (Anti-inflammatory) group received IS-741 intraperitoneally from Day -7 to Day 14 and intratracheal BLM injection; and (F) the BLM + IS-741 (Anti-fibrotic) group received IS-741 intraperitoneally from Day 14 to Day 28 and intratracheal BLM injection. To examine the time kinetics of the effects of IS-741, mice were treated separately with IS-741 from Days -7 to 14 (early treatment = Anti-inflammatory) or Days 14 to 28 (late treatment = Anti-fibrotic), as previously described [16, 17]. For examination, the mice were killed by drawing blood from the right atrium under anesthesia. Bronchoalveolar lavage (BAL) and histopathology were performed on Day 7. Hydroxyproline assay, histopathological examinations, and measurement of fluid content were performed on surviving mice on Day 28. The experiments of the sampling at Day 7 and the sampling at Day 28 were performed independently, as described in Fig. 1.

Morphological Evaluation

The right lung was removed with the left main bronchus ligation and fixed by filling the lung through a tracheal cannula to 25 cmH_2O with 10% neutral buffered formaldehyde solution. The trachea was then occluded and fixation was allowed to continue for 4–10 days prior to the study. Longitudinal tissue sections of the lung were embedded in paraffin, stained with hematoxylin-eosin (HE), and examined by light microscopy at a magnification of ×100. Each histopathological experiment was performed in at least three or four mice per group.

Measurement of Hydroxyproline or Fluid Content of the Lung

Hydroxyproline content (μg/lung) in the left lung of each subject was assayed according to the commonly used procedure of colorimetric measurement (Mitsubishi Kagaku Bio-Clinical Laboratories, Inc., Tokyo, Japan). Briefly, lungs were harvested on each designated day after BLM administration and homogenized in 1 ml of PBS (pH 7.4) with a tissue tearer. A 1.5-ml volume of each sample (left lung) was then digested in 1 ml of 6 N hydrochloric acid (HCl) for 8 h at 120°C. Five microliters of citrate-acetate buffer (5% citric acid, 7.24% sodium acetate, 3.4% sodium hydroxide, and 1.2% glacial acetic acid, pH 6.0)

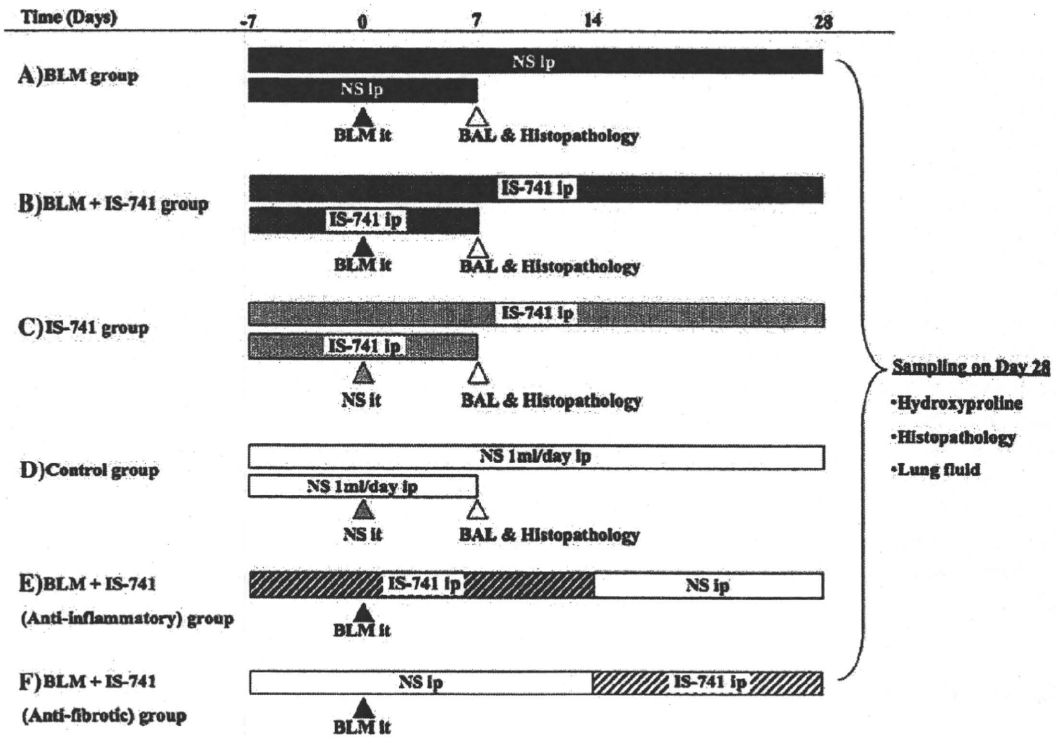

Fig. 1 Experimental designs to determine the activity of IS-741 as an inhibitory agent in the bleomycin (BLM) model. Mice were intratracheally (it) administered BLM or normal saline (NS). IS-741 was administered intraperitoneally (ip). The BLM group received intratracheal BLM injection (A). The BLM + IS-741 group received IS-741 for 5 weeks (B). The IS-741 group (C) and the Control group (D) received intratracheal NS injections. The BLM + IS-741 (Anti-inflammatory) group received IS-741 from Day -7 to Day 14 (E). The BLM + IS-741 (Anti-fibrotic) group received IS-741 from Day 14 to Day 28 (F). The samplings of bronchoalveolar lavage (BAL) fluid at Day 7 and hydroxyproline contents at Day 28 were performed as independent studies

and 100 ml of chloramine-T solution (282 mg of chloramines-T, 2 ml of *n*-propanol, 2 ml of H_2O, and 16 ml of citrate-acetate buffer) were added to each 5-ml sample and the samples were left at room temperature for 20 min. Next, 100 ml of Ehrlich's solution, 9.3 ml of *n*-propanol, and 3.9 ml of 70% perchloric acid were added to each sample and the samples were incubated for 15 min at 65°C. Samples were cooled for 10 min and read at 550 nm on a spectrophotometer. Hydroxyproline concentrations from 0 to 400 mg/ml were utilized to construct a standard curve.

The wet lung weight of the left lobe was measured after careful excision of extraneous tissues. The lung was exposed for 48 h at 180°C and the dry weight measured. Water content was calculated by subtraction of the dry weight from the wet weight.

Sampling of BAL Fluid

BAL was performed through a tracheal cannula to the right lung with 0.5 ml of saline four times, with the left main bronchus ligation. In each mouse examined, approximately 1.8 ml (90%) of BAL fluid (BALF) was recovered. A 100-μl aliquot was used for the total cell count, and the remainder was immediately centrifuged at 1000 *g* for 10 min. The total cell count was made using a hemocytometer, and cell differentiation was determined for more than 500 cells on cytocentrifuge slides with Wright-Giemsa staining. The supernatants of BALF were stored at −80°C until used.

Assays for $cPLA_2$ Products and MCP-1 in BALF

Thromboxane (Tx) A_2 measured as TxB_2, leukotriene (LT) B_4, and cysteinyl leukotrienes (cysLTs) in BALF were determined by using enzyme immunoassay (EIA) kits (Amersham Pharmacia Biotech, Piscataway, NJ, USA). MCP-1 in BALF was measured by the Mouse MCP-1 Immunoassay kit (Biosource International, Camarillo, CA, USA).

Flow Cytometry of LFA-1 (CD11a/CD18) in BAL Cells

Suspended BAL cells in PBS from the three groups (the BLM group, the BLM + IS-741 group, and the Control

group) were stained with fluorescein isothiocyanate-, phycoerythrin-, or pericinin chlorophyll protein-conjugated monoclonal anti-CD11a, CD18, and CD45 antibodies (Becton-Dickinson, San Jose, CA, USA) in phosphate buffer saline for 20 min at 4°C. Stained cells were analyzed on flow cytometry (FACScan; Becton-Dickinson) using a Cell Quest program. Leukocytes were determined using flow cytometric analysis of light scatter chamber characteristics relating to size and granulation, and fluorescence gating with anti-CD45 antibody. Three-color flow cytometry was then performed to calculate the percentages of CD11a and CD18 positive cells in a subset of $CD45^+$ leukocytes.

Statistical Analysis

Survival curves were estimated by the Kaplan–Meier method. Comparisons of all curves were done using the two-tailed log-rank test. Data were expressed as mean ± SEM. For multiple comparisons, we performed a one-way analysis of variance, and then Fisher's protected least-significant differences method was used as a post-hoc test. Values of $P < 0.05$ were considered to indicate statistical significance.

Results

Effects of IS-741 on Mortality in BLM-Treated Mice

Contrary to our expectation, there was no significant difference in the survival rate on Day 28 between the BLM group and the BLM + IS-741 group ($P > 0.05$; 80% vs. 87%, respectively), using a two-tailed log-rank test (Fig. 2). The Control group and the IS-741 group recorded no deaths (Fig. 2).

Analysis of Inflammatory Cell Infiltration to the Lung by Instillation of BLM

Inflammatory cell infiltration into the lung was evaluated by histologic examination and BALF cell analysis on Day 7. Edematous thickening of alveolar septa and the infiltration of neutrophils and macrophages and a few lymphocytes were observed by BLM instillation (Fig. 3a). The alveolitis was less severe in the BLM + IS-741 group than in the BLM group (Fig. 3a, b).

Preadministration of IS-741 significantly reduced the number of total cells in the BALF ($P = 0.018$) (Fig. 3e). In the BALF cell differentiation, macrophages, neutrophils, and lymphocytes tended to be reduced by IS-741 but not significantly (Fig. 3e).

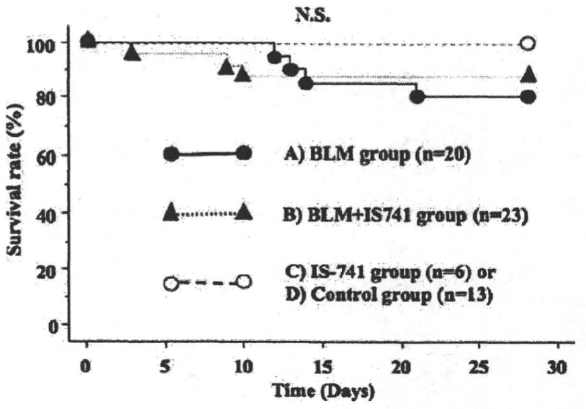

Fig. 2 Effects of IS-741 on mortality in the bleomycin (BLM) model. The survival rates of four study groups of mice are shown over a 28-day observation period. There was no significant difference among the BLM group (●), the BLM + IS-741 group (▲), and the IS-741 group or the control group (○). The described number of each group was a pool of three independent experiments

Administration of IS-741 Ameliorated BLM-Induced Pulmonary Fibrosis or Lung Edema in Mice

The fibrotic change in the lung was evaluated by histological examination and measurement of hydroxyproline contents. As shown in Fig. 4a–f, all three IS-741 administration groups demonstrated significant reduction of fibrosis in the subpleural areas or the around bronchiole of the lung. IS-741 has been reported to be the anti-inflammatory agent, as described above. However, in addition to histologic examination, the hydroxyproline assay demonstrated that IS-741 reduced the total hydroxyproline contents in all three treated groups compared with the BLM-alone group (Fig. 4g).

To evaluate lung edema formation, we measured wet-dry lung weight. Compared with the BLM group, the BLM + IS-741 group significantly reduced the fluid content (Fig. 5).

Effects of IS-741 on the $cPLA_2$ Products and MCP-1 Levels in BALF of the BLM Model

To assess the biosynthesis of $cPLA_2$ products we performed BALF assays of TxB_2, LTB_4, and cysLTs (LTC_4/D_4/E_4). As shown in Fig. 6a, cysLTs level in BLM-treated mice was significantly greater than that in the two groups that did not receive BLM. However, pretreatment with IS-741 significantly decreased the elevated levels of cysLTs in BALF compared with those in the animals treated with BLM alone ($P = 0.006$). For other eicosanoids, BALF levels of TxB_2 or LTB_4 in the BLM + IS-741 group did not differ from those in the BLM group (data not shown).

The MCP-1 level in BALF was measured as an index of the amount of regulating factor of monocyte chemoattractant and infiltration to the lung. As shown in Fig. 6b, the

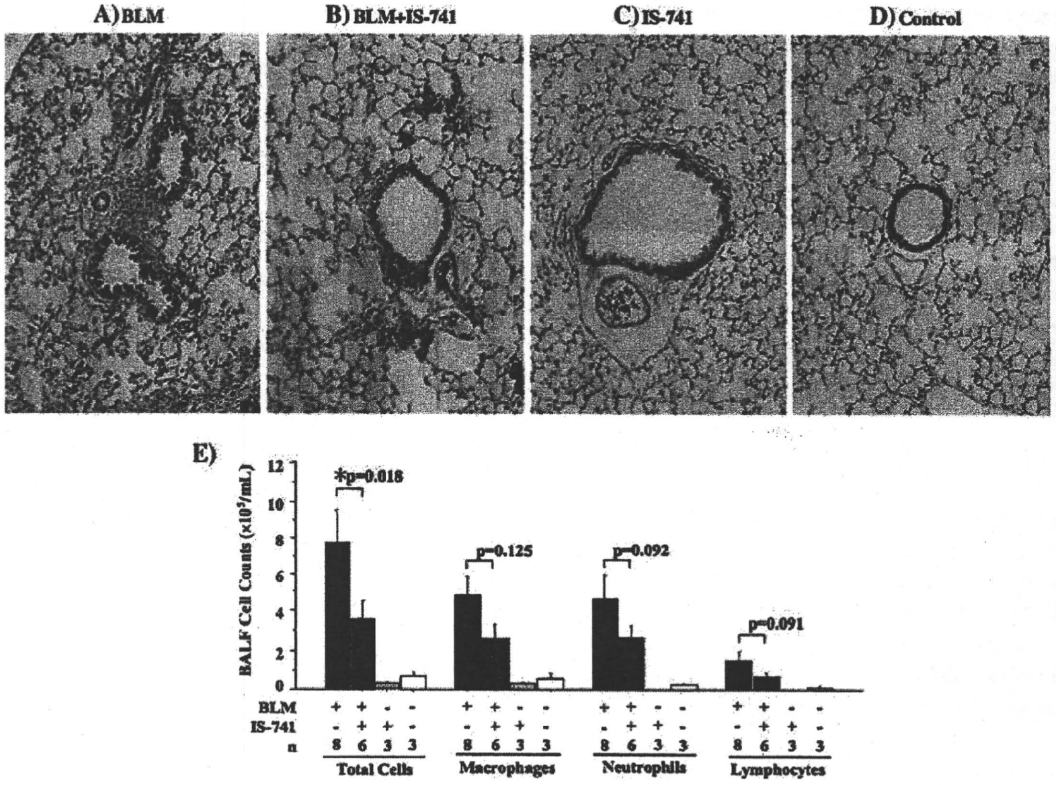

Fig. 3 Effects of IS-741 on acute inflammatory phase in the bleomycin (BLM) model. Lung tissue was obtained on Day 7 and stained with hematoxylin and eosin (original magnification ×100). Alveolar thickening and infiltration of inflammatory cells in the alveolar space are seen in the BLM group (**a**); however, these features are less severe in the BLM + IS-741group (**b**). No histological effect on the lung tissue is observed in the IS-741 group (**c**) compared with the Control group (**d**). On bronchoalveolar lavage fluid findings at Day 7, the number of total cells in the BLM + IS-741 group is significantly decreased compared with that in the BLM group (**e**). No differences have been seen in the IS-741 group compared with the Control group (**e**). Data are presented as the mean ± SEM. $*P < 0.05$ in comparison to the BLM group. Data are representative of three separate experiments

preadministration of IS-741 caused a significant reduction of the elevated levels of MCP-1 in BALF induced by BLM challenge ($P = 0.037$).

Flow Cytometry of LFA-1 (CD11a/CD18) in BAL Cells

Inflammatory cells from BAL were analyzed by flow cytometry to evaluate the expression of surface antigens CD11a and CD18. Although the frequency of $CD11a^+$ or $CD18^+$ cells from BAL of the BLM group was greater than that of the Control group, administration of IS-741 did not affect the percentage of $CD11a^+$ or $CD18^+$ cells from BAL (data not shown).

Discussion

In the present study, a murine BLM-induced pulmonary fibrosis mouse model was used to examine the ability of IS-741 to inhibit pulmonary fibrosis by decreasing lung inflammation and attenuating $cPLA_2$ products or MCP-1 levels. We have shown that IS-741 could mitigate the progression of lung injury and fibrosis. It also attenuated the cellular infiltration and the concentrations of cysLTs and MCP-1 in BALF. These findings suggested that IS-741 could inhibit lung injury and fibrosis via the repression of cysLTs or MCP-1 production in the current model.

A major difference between human IPF and the mouse model is the inflammatory component of early BLM-induced lung injury, which is often absent in human IPF [18]. Chaudhary et al. [19] determined the time course of the development of inflammation and fibrosis in BLM-induced lung fibrosis in rat. They demonstrated that in an animal model that comprised a single intratracheal injection of BLM, the "switch" between inflammation and fibrosis occurred on or just after Day 9 [19]. At first we hypothesized that IS-741 has an only "anti-inflammatory" effect. Despite our expectation, not only the "Anti-inflammatory" group but also the "Anti-fibrotic" group

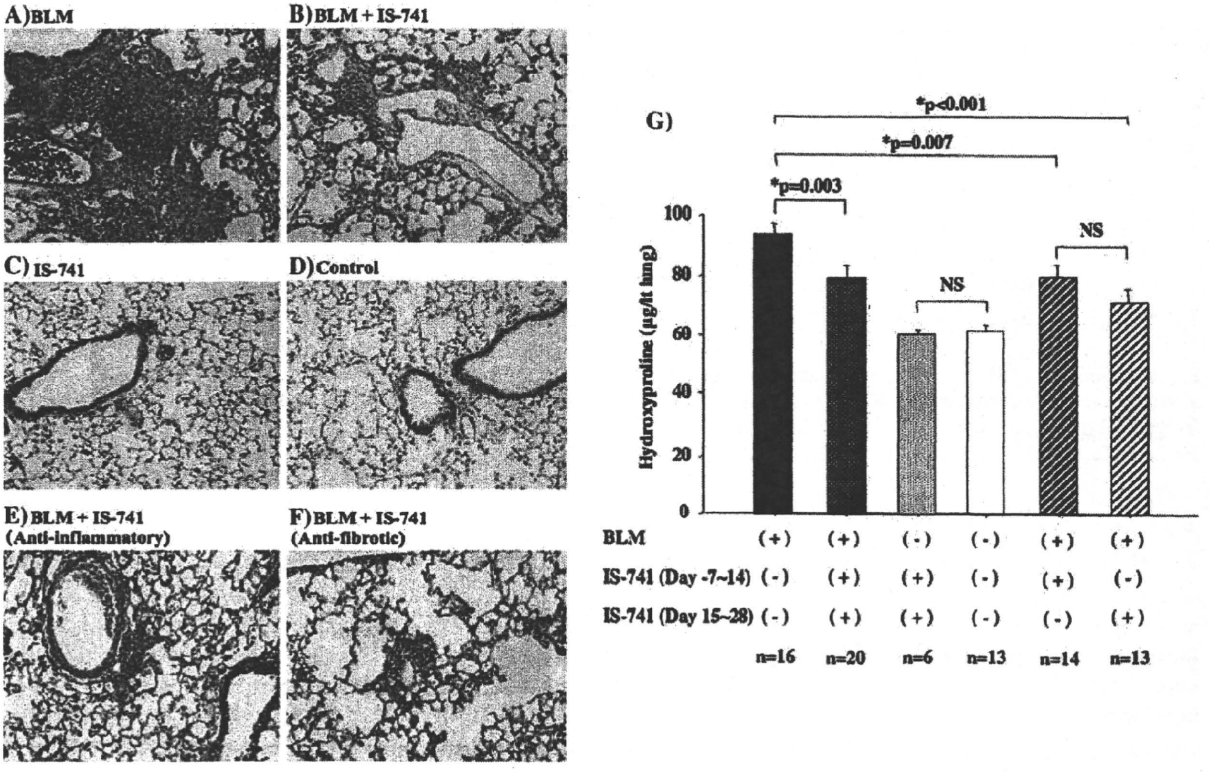

Fig. 4 Effects of IS-741 on chronic fibrotic phase in the bleomycin (BLM) model. Lung tissue was obtained on Day 28 after instillation of BLM or saline and stained with hematoxylin and eosin (original magnification ×100). A lung tissue sample from the BLM group shows alveolitis and patchy fibrosis with destruction of the alveolar structure, mainly in the bronchiole region (**a**). However, these features are less severe in the three IS-741 treatment groups: the BLM + IS-741 group (**b**), the BLM + IS-741 (Anti-inflammatory) group (**e**), and the BLM + IS-741 (Anti-fibrotic) group (**f**). A lung tissue sample from the IS-741 group (**c**) and the Control group (**d**) appear normal. Data are representative of three separate experiments. The BLM + IS-741 group significantly attenuates the BLM-induced increase in hydroxyproline content on Day 28 (**g**). In addition, the BLM + IS-741 (Anti-inflammatory) group and the BLM + IS-741 (Anti-fibrotic) group also significantly decrease hydroxyproline contents (**g**). Data are presented as the mean ± SEM (n = 6–20 in each group). *$P < 0.05$ in comparison to the BLM group. The described number of each group was a pool of three independent experiments. Details of each group protocol are described in Fig. 1

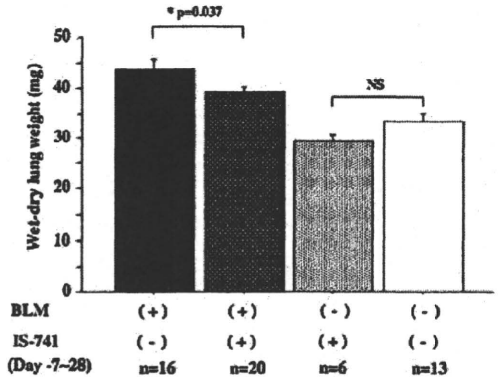

Fig. 5 Effects of IS-741 on fluid contents of the bleomycin (BLM) model. Treatment with IS-741 from Day -7 to Day 28 significantly reduced edema formation induced by BLM. Data are presented as mean ± SEM. The described number of each group was a pool of three independent experiments

could mitigate the progression of pulmonary fibrosis. There are two previous reports on the therapeutic (not preventive) effect of IS-741 on chronic pancreatic fibrosis models [15, 20]. In those studies, to exclude the effect of IS-741 on acute pancreatitis and to evaluate the efficacy on the chronic phase the authors started administration of IS-741 at Day 7 or later after the challenge of dibutyltin dichloride or dibutyltin dichloride, respectively [15, 20]. They reported that pancreatic fibrosis was inhibited by IS-741 administration therapeutically [15, 20]. In vitro study has shown that IS-741 had no direct effect on the proliferation, collagen synthesis, or α smooth muscle actin expression of rat pancreatic stellate cells without MCP-1 production [15]. Further analysis will be needed to determine which cells affect MCP-1 production by IS-741 in the fibrotic lung.

It has been reported that the MCP-1 functional pathway may play an important role in the development of pulmonary fibrosis [21–25]. Although our results indicated

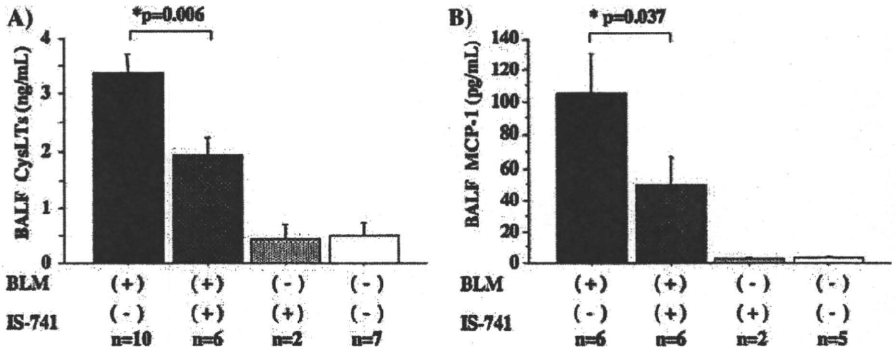

Fig. 6 Effects of IS-741 on the cysteinyl leukotrienes (cysLTs) and monocyte chemoattractant protein (MCP)-1 levels in bronchoalveolar lavage fluid (BALF) in the bleomycin (BLM) model. BALF levels of both cysLTs (**a**) and MCP-1 (**b**) are significantly attenuated in the BLM + IS-741 group in comparison to the BLM group on Day 7. Data are presented as the mean ± SEM. * $P < 0.05$ compared with the BLM group. Data are representative of three separate experiments

that IS-741 might regulate MCP-1 production in the lung of the BLM-induced pulmonary fibrosis model, the exact mechanism of IS-741 responsible for this inhibitory action at the chronic fibrosis phase has not yet been elucidated. Inoshima et al. [26] have shown that overexpression of a mutant MCP-1 gene 10–14 days after intratracheal BLM instillation resulted in decreased DNA damage, apoptosis, and pulmonary fibrosis at 14 days. However, overexpression of the mutant MCP-1 0–4 days after BLM instillation did not decrease the pathological grade, DNA damage, or apoptosis at 7 and 14 days [26]. These findings suggest that MCP-1 might play an important role in the development of fibrogenesis but not in the development of early lung inflammation. Further examination is needed to clarify the antifibrotic function of IS-741 in lung fibrosis.

BLM-induced lung fibrosis was significantly reduced in the 5-lipoxygenase knockout mouse or the $cPLA_2$ knockout mouse by inhibiting cysLTs [27, 28]. These findings suggest that $cPLA_2$ products may have a pivotal role in the development of pulmonary fibrosis. Originally, IS-741 was prepared and evaluated as a $cPLA_2$ inhibitor; however, a high concentration was needed to inhibit $cPLA_2$ activity [7, 8]. The present study demonstrated that IS-741 reduced the elevated levels of cysLTs in BALF. The reduction of cysLTs might mainly be a secondary effect because of the attenuation of the infiltration of inflammatory cells into the lung. In addition, $cPLA_2$-inhibiting activity of IS-741 may also attenuate the production of cysLTs.

Many adhesion molecules are crucial for securing leukocyte-endothelial cell interaction such as the selectin family; the immunoglobulin superfamily, including intercellular adhesion molecule 1 and vascular cell adhesion molecule 1; and the integrin family, including LFA-1, Mac-1, and very late antigen 4 [29]. IS-741 has an inhibitory action against the cell adhesion between leukocytes and microvascular endothelial cells [10, 12, 30]. IS-741 has been reported to inhibit cell adhesion significantly between human umbilical vein endothelial cells and human promyeloleukemia cells during lipopolysaccharide stimulation in vitro [31]. It has been suggested that the exact mechanism of IS-741 responsible for this inhibitory action is that IS-741 inhibits the cluster formation of LFA-1 with the activation of LFA-1 [32]. Our flow cytometry analysis showed that administration of IS-741 did not affect the percentage of $CD11a^+$ or $CD18^+$ cells from BAL in our model. This finding may the support the above hypothesis that IS-741 did not affect the amounts of LFA-1 expression but inhibited the cluster formation of activating LFA-1. Although anti-inflammatory effects of IS-741 on acute inflammation with the infiltration of leukocytes were reported [9, 10, 12–14], effects of IS-741 on chronic inflammation and fibrosis remain unclear.

Yotsuya et al. [33] have shown that the number of infiltrating leukocytes on acute pancreatitis in rats was significantly decreased after treatment with10 mg/kg/day of IS-741 but not after 0.1 or 1 mg/kg/day of IS-741. Therefore, we used IS-741 at a dose of 10 mg/kg/day. Although most studies used 10 mg/kg/day of IS-741 [9, 10, 12, 14], the other studies used IS-741 in large quantities such as 20 mg/kg/day in dogs [8] and 50 mg/kg/day [13, 15], 72 mg/kg/day [11], and 100 mg/kg/day [32] in rats. As shown in Fig. 1, four of 20 mice (20%) in the BLM group died, and three of 23 mice (13%) in the BLM + IS741 group died. One could conclude that the beneficial effects of IS-741 are not significant. We did not explain the exact reason why administration of IS-741 did not affect mortality, but our dose of IS-741 might be slightly small to show the statistically significant attenuation of mortality.

In summary, the results of the present study suggested that IS-741 could inhibit BLM-induced lung injury and fibrosis by the repression of MCP-1 and cysLTs production. These findings suggested that the administration of IS-

741 might therefore modulate the process of pulmonary fibrosis via regulating anti-inflammatory mediator production. However, the precise mechanism by which IS-741 modulates lung injury and/or fibrosis remains obscure. Further studies are thus required to elucidate this issue.

Acknowledgments This study was supported by the Health and Labour Sciences Research Grants on Diffuse Lung Diseases from the Japanese Ministry of Health, Labour and Welfare, Grant for Promotion of Niigata University Research Projects (90), and Research Grant from Shimane University Medical School Alumni Association.

References

1. Kuwahara F, Kai H, Tokuda K, Niiyama H, Tahara N, Kusaba K, Takemiya K, Jalalidin A, Koga M, Nagata T, Shibata R, Imaizumi T (2003) Roles of intercellular adhesion molecule-1 in hypertensive cardiac remodeling. Hypertension 41:819–823
2. Chow FY, Nikolic-Paterson DJ, Ozols E, Atkins RC, Tesch GH (2005) Intercellular adhesion molecule-1 deficiency is protective against nephropathy in type 2 diabetic db/db mice. J Am Soc Nephrol 16:1711–1722
3. Blaber R, Stylianou E, Clayton A, Steadman R (2003) Selective regulation of ICAM-1 and RANTES gene expression after ICAM-1 ligation on human renal fibroblasts. J Am Soc Nephrol 14:116–127
4. Imamura M, Ogawa T, Sasaguri Y, Chayama K, Ueno H (2005) Suppression of macrophage infiltration inhibits activation of hepatic stellate cells and liver fibrogenesis in rats. Gastroenterology 128:138–146
5. Huo Y, Ley K (2001) Adhesion molecules and atherogenesis. Acta Physiol Scand 173:35–43
6. American Thoracic Society (2000) Idiopathic pulmonary fibrosis: diagnosis and treatment. International consensus statement. American Thoracic Society (ATS), and the European Respiratory Society (ERS). Am J Respir Crit Care Med 161:646–664
7. Kimura H, Yotsuya S, Yuki S, Sugi H, Shigehara I, Haga T (1995) Synthesis and antipancreatitis activities of novel N-(2-sulfonylamino-5-trifluoromethyl-3-pyridyl) carboxamide derivatives as phospholipase A2 inhibitors. Chem Pharm Bull (Tokyo) 43:1696–1700
8. Isaji S, Hayashi J, Higashiguchi T, Yokoi H, Ogura Y, Noguchi T, Kawarada Y (1999) Effect of IS-741 (a new synthetic antiinflammatory agent) on acute necrotizing pancreatitis in dogs. Significance of its inhibitory effect on cytosolic phospholipase A2. Digestion 60(Suppl 1):47–51
9. Makino J, Andoh A, Hata K, Yotsuya S, Shikama H, Araki Y, Fujiyama Y, Bamba T (2002) Suppressive effects of a new anti-inflammatory agent, IS-741, on dextran sulfate sodium-induced experimental colitis in rats. Int J Mol Med 9:391–396
10. Yamauchi J, Sunamura M, Shibuya K, Takeda K, Kobari M, Matsuno S (1999) A novel diamino-pyridine derivative prevents excessive leukocyte infiltration in aggravation of acute necrotizing pancreatitis. Digestion 60(Suppl 1):40–46
11. Yamaguchi Y, Okabe K, Liang J, Matsumura F, Akizuki E, Matsuda T, Ohshiro H, Nakano S, Ishihara K, Ogawa M (1999) The novel carboxamide derivative IS-741 reduces neutrophil chemoattractant production by bronchoalveolar macrophages in rats with cerulein-induced pancreatitis complicated by sepsis. Digestion 60(Suppl 1):52–56
12. Imamura T, Niikawa J, Kitamura K, Takahashi A, Ikegami A, Yoshida H, Tanaka S, Mitamura K (2003) Effect of IS-741 on ethionine-induced acute pancreatitis in rats: relation to pancreatic acinar cell regeneration. J Gastroenterol 38:260–267
13. Fukunaga T, Tsujikawa T, Sasaki M, Fujiyama Y, Bamba T, Fujimiya M (2003) A novel diamino-pyridine derivative (IS-741) attenuates rat ileitis induced by trinitrobenzene sulfonic acid. J Gastroenterol 38:451–459
14. Makino J, Andoh A, Hata K, Yotsuya S, Shikama H, Imamura M, Fujiyama Y, Bamba T (2002) Inhibitory effects of the new anti-inflammatory agent, IS-741, on spontaneous colitis in HLA-B27/beta2-microglobulin transgenic rats. J Gastroenterol Hepatol 17:854–860
15. Kaku T, Oono T, Zhao H, Gibo J, Kawabe K, Ito T, Takayanagi R (2007) IS-741 attenuates local migration of monocytes and subsequent pancreatic fibrosis in experimental chronic pancreatitis induced by dibutyltin dichloride in rats. Pancreas 34:299–309
16. Aono Y, Nishioka Y, Inayama M, Ugai M, Kishi J, Uehara H, Izumi K, Sone S (2005) Imatinib as a novel antifibrotic agent in bleomycin-induced pulmonary fibrosis in mice. Am J Respir Crit Care Med 171:1279–1285
17. Azuma M, Nishioka Y, Aono Y, Inayama M, Makino H, Kishi J, Shono M, Kinoshita K, Uehara H, Ogushi F, Izumi K, Sone S (2007) Role of alpha1-acid glycoprotein in therapeutic antifibrotic effects of imatinib with macrolides in mice. Am J Respir Crit Care Med 176:1243–1250
18. Selman M, King TE, Pardo A (2001) Idiopathic pulmonary fibrosis: prevailing and evolving hypotheses about its pathogenesis and implications for therapy. Ann Intern Med 134:136–151
19. Chaudhary NI, Schnapp A, Park JE (2006) Pharmacologic differentiation of inflammation and fibrosis in the rat bleomycin model. Am J Respir Crit Care Med 173:769–776
20. Xie MJ, Motoo Y, Su SB, Iovanna JL, Sawabu N (2002) Effect of carboxamide derivative IS-741 on rat spontaneous chronic pancreatitis. Dig Dis Sci 47:139–147
21. Antoniades HN, Neville-Golden J, Galanopoulos T, Kradin RL, Valente AJ, Graves DT (1992) Expression of monocyte chemoattractant protein-1 mRNA in human idiopathic pulmonary fibrosis. Proc Natl Acad Sci USA 89:5371–5375
22. Iyonaga K, Takeya M, Saita N, Sakamoto O, Yoshimura T, Ando M, Takahashi K (1994) Monocyte chemoattractant protein-1 in idiopathic pulmonary fibrosis and other interstitial lung diseases. Hum Pathol 25:455–463
23. Car BD, Meloni F, Luisetti M, Semenzato G, Gialdroni-Grassi G, Walz A (1994) Elevated IL-8 and MCP-1 in the bronchoalveolar lavage fluid of patients with idiopathic pulmonary fibrosis and pulmonary sarcoidosis. Am J Respir Crit Care Med 149:655–659
24. Suga M, Iyonaga K, Ichiyasu H, Saita N, Yamasaki H, Ando M (1999) Clinical significance of MCP-1 levels in BALF and serum in patients with interstitial lung diseases. Eur Respir J 14:376–382
25. Zhang K, Gharaee-Kermani M, Jones ML, Warren JS, Phan SH (1994) Lung monocyte chemoattractant protein-1 gene expression in bleomycin induced pulmonary fibrosis. J Immunol 153:4733–4741
26. Inoshima I, Kuwano K, Hamada N, Hagimoto N, Yoshimi M, Maeyama T, Takeshita A, Kitamoto S, Egashira K, Hara N (2004) Anti-monocyte chemoattractant protein-1 gene therapy attenuates pulmonary fibrosis in mice. Am J Physiol Lung Cell Mol Physiol 286:L1038–L1044
27. Peters-Golden M, Bailie M, Marshall T, Wilke C, Phan SH, Toews GB, Moore BB (2002) Protection from pulmonary fibrosis in leukotriene-deficient mice. Am J Respir Crit Care Med 165:229–235
28. Nagase T, Uozumi N, Ishii S, Kita Y, Yamamoto H, Ohga E, Ouchi Y, Shimizu T (2002) A pivotal role of cytosolic phospholipase A(2) in bleomycin-induced pulmonary fibrosis. Nat Med 8:480–484
29. Salmi M, Jalkanen S (2005) Cell-surface enzymes in control of leukocyte trafficking. Nat Rev Immunol 5:760–771